NOVA SCHOOL OF SCIENCE & TECHNOLOGY

DEPARTAMENT OF LIFE SCIENCES

BEATRIZ LUÍS PEREIRA

BSc in Cell and Molecular Biology

NEW INSIGHTS ON THE PATHOMECHANISM OF GNE MYOPATHY: PROPOSING AN IMMUNE-MEDIATED RESPONSE

MASTER IN MOLECULAR GENETICS AND BIOMEDICINE

NOVA University Lisbon

September, 2022

DEPARTAMENT OF
LIFE SCIENCES

NEW INSIGHTS ON THE PATHOMECHANISM OF GNE MYOPATHY: PROPOSING AN IMMUNE-MEDIATED RESPONSE

BEATRIZ LUÍS PEREIRA

BSc in Cell and Molecular Biology

Adviser: Paula Videira
Assistant Professor, NOVA University Lisbon

Co-adviser: Mariana Barbosa
Postdoctoral Researcher, NOVA University Lisbon

Examination Committee:

Chair: Margarida Castro-Caldas

Rapporteurs: Tiago Ferro

Adviser: Paula Videira

MASTER IN MOLECULAR GENETICS AND BIOMEDICINE

NOVA University Lisbon
September, 2022

New insights on the pathomechanism of GNE myopathy: proposing an immune-mediated response

The work developed during this master project has originated:

- **Oral communications:**

1. Pereira, BL; Barbosa, M; Videira, PA. The ProDGNE project: Getting to know the research and the disease. 10º Congresso Português de Doenças Neuromusculares, 30th September – 1st October, Aveiro, Portugal, 2022.
2. Barbosa, M; Pereira, BL; Videira, PA. Targeting imune-mediated responses to tackle GNE myopathy. Biosystems in Toxicology and Pharmacology – Current challenges, 8th – 9th September, Virtual, 2022.
3. Barbosa, M; Pereira, F; Pereira, BL; Serpi, M; Pertusati, F; Videira, PA; Phosphate prodrug technology: Pursuing a new therapeutic approach for GNE myopathy. 14th National Organic Chemistry Meeting & 7th National Medicinal Chemistry Meeting, 20th – 22nd April, Caparica, Portugal, 2022.
4. Francisco R, Brasil S, Pascoal C, Marques-da-Silva D, Pimentel-Santos FM, Barbosa M, Pereira BL, Jaeken J, Grosso AR, Ferreira V, Videira PA. CDG&Allies-PPAIN: A patient-led initiative aiming to unravel the role of immunological and skeletal manifestations in Congenital Disorders of Glycosylation. 12 Topics in Rheumatology, 3rd Edition, 30th September – 2nd October, Lisbon, Portugal, 2021.

- **Posters:**

1. Pereira, BL; Barbosa, M; Videira, PA. Expanding knowledge on a rare Congenital Disorder of Glycosylation: GNE myopathy. iMED Conference® 14.0, 12-16th October, Lisbon, Portugal, 2022 (*selected*).
2. Pereira, BL; Barbosa, M; Rabaça, J; Silva, Z; Videira, PA. Antigen presentation: An evidence of immune-mediated response in GNE myopathy? European Conference on Rare Diseases, 27th June – 1st July, Virtual, 2022.
3. Pereira, BL; Barbosa, M; Videira, PA. New insights on GNE myopathy pathomechanisms. ProDGNE Meeting 2022, 31st May – 1st June, Caparica, Portugal, 2022.

- **Publications:**

1. Barbosa, M; Pereira, BL; Videira, PA. Targeting imune-mediated responses to tackle GNE myopathy. *Med. Sci. Forum* **11**, 9 (2022). https://doi.org/10.3390/BiTaP-12788
2. Barbosa, M; Pereira, F; Pereira, BL; Serpi, M; Pertusati, F; Videira, PA. Phosphate prodrug technology: Pursuing a new therapeutic approach for GNE myopathy, 14th Edition of the Nacional Organic Chemistry Meeting and 7th Edition of the Nacional Therapeutic Chemistry Meeting. *Chem. Proc.* **11**, 30-31 (2022). https://doi.org/10.3390/chemproc2022011001

Acknowledgements

I would like to start by thanking to Professor Paula Videira for giving me the opportunity to work in the Glycoimmunology group and for all the insights, guidance and advice given since my first day in the laboratory.

I would like to give a special thanks to Mariana Barbosa, firstly, for accepting co-supervision my dissertation. Secondly, for all the daily support in the lab, for all the knowledge shared and encouragement. And, last but not least, for all our funny moments, inside jokes, Brazilian funks, rides to Lisbon and for the amazing friendship that I know will last.

A big thank you to Daniela Barreira, Carlota Pascoal and Rita Lourenço for all the help during this year, the good moments, such as our snack times, our plans and trips to the beach and for the friendship.

I could not fail to thank Ana Sofia Rodrigues, because I never thought I would find someone so special during this year. Someone with the same interests as me and with the ambition to explore a future in research. It was amazing to share this experience with her.

I am sincerely grateful to Danielle Almeida for all the cheerful, life lessons and for always having a friendly word.

I also want to thank all my other lab members: Zélia Silva, Pedro Granjo, João Rabaça and Rita Francisco, for all the support and moments shared.

To my dear friends: João Pedro, Tânia, Madalena and Maria Manuel for making me believe in my worth throughout this journey. I must also thank my girls from Muchachas and my friend Johnny for always being ready for going out and talk.

My biggest thanks goes to my boyfriend, João, who more than anyone else accompanied me this year, and above all understands what I am going through.

Lastly, to my precious family, namely my cousin Catarina, who went through similar awkward conversations about the thesis progress, and especially to my parents, for all the support and for making me believe that I can be anything I want.

“Just because it won't come easily
Doesn't mean we shouldn't try”

Bruno Major

Abstract

Glycosylation is known to be involved in several biological functions, and defects in the synthesis or attachment of sugars can modulate the course of various malignancies. GNE myopathy (GNEM) is an ultra-rare congenital disorder of glycosylation caused by biallelic mutations in the *GNE* gene, which encodes for a bifunctional enzyme required for sialic acid biosynthesis. Although, hyposialylation has been assumed as the main cause of this myopathy, new data suggest that GNEM mechanism is far more complicated. To date, there is no approved treatment for GNEM and research on sialylation-increasing therapies is challenged by unknown processes and the absence of biomarkers.

In this work we explored cellular and molecular mechanisms that may contribute to this myopathy as a means of identifying alternative therapeutic targets and biomarkers. Previous studies have identified that sialic acid removal alters the expression of some immune agents; this led us to study whether defective sialylation in the *GNE* knock-out cell model influences immune function. The overexpression of major histocompatibility complex class-I (MHC-I) and cytokine secretion levels in GNEM cell model point towards the involvement of an immune response and suggest that immune players could be good disease biomarkers in diagnostic and clinical development.

Furthermore, drug-likeliness of newly synthesized compounds (based on prodrug technology) was computationally analysed, and assays to evaluate the *in vitro* toxicity and efficacy of the prodrugs were designed and optimized, using *N*-acetyl-D-mannosamine currently in phase 2 of clinical trials and *N*-acetyl-D-mannosamine-6-phosphate (parent compound). Although no restoring of the sialic acid content was observed with both compounds, a small recovery of immune parameters suggests the involvement of pathways other than sialylation.

Overall, understanding the immune response in GNEM could bring some light into pathophysiology and accelerate the approval of a new therapeutic option.

Keywords: Glycosylation, Sialic acid, Congenital Disorders of Glycosylation, GNE myopathy, Biomarkers, and Prodrugs.

Resumo

A glicosilação está envolvida em várias funções biológicas. Defeitos na síntese ou fixação de monossacáridos podem modular o desenvolvimento de várias doenças. A miopatia GNE (GNEM) é uma doença congénita da glicosilação ultra-rara causada por mutações bialélicas no gene *GNE*, que codifica uma enzima bifuncional crucial para a biossíntese de ácido siálico. Embora se assuma a hiposialilação como a principal causa desta miopatia, novas evidências sugerem que o mecanismo de doença é mais complexo. Atualmente, não existe nenhum tratamento aprovado para GNEM e a investigação em torno de terapias que aumentam a sialilação é dificultada por mecanismos desconhecidos e ausência de biomarcadores.

Neste trabalho explorámos mecanismos que podem contribuir para a GNEM no sentido de identificar alvos terapêuticos alternativos e biomarcadores. Estudos anteriores identificaram que a remoção de ácido siálico altera a expressão de alguns agentes imunes, o que nos levou a estudar se a função imune está alterada no modelo celular com o gene *GNE* knock-out. A sobre-expressão do complexo principal de histocompatibilidade classe I (MHC-I) e os níveis de secreção de citocinas observados no modelo celular de GNEM apontam para o envolvimento de uma resposta imune e sugerem que moléculas imunes podem ser bons biomarcadores no diagnóstico e desenvolvimento clínico.

Além disso, as propriedades "drug-like" de novos compostos sintetizados (pró-fármacos) foram analisadas computacionalmente, e ensaios *in vitro* para avaliar a toxicidade e a eficácia dos pró-fármacos foram otimizados, usando *N*-acetil-D-manosamina atualmente na fase 2 de ensaios clínicos e *N*-acetil-D-manosamina-6-fosfato (princípio ativo). Embora nenhuma recuperação da sialilação tenha sido observada com os compostos, houve uma pequena recuperação dos parâmetros imunológicos, sugerindo o envolvimento de outras vias além da sialilação.

Em jeito de conclusão, entender a resposta imune na GNEM pode trazer mais entendimento da sua fisiopatologia e acelerar a aprovação de novas e melhores opções terapêuticas.

Palavras-chave: Glicosilação, Ácido siálico, Doenças Congénitas da Glicosilação, Miopatia GNE, Biomarcadores e Pró-fármacos.

Index of Contents

Index of Figures

Appendix

Index of Tables

List of Abbreviations

AAV8	Adeno-associated Viruses 8
Ace-ER	Extended-release Formulation of Neu5Ac
ADMET	Absorption, Distribution, Metabolization, Excretion and Toxicity
APC	Allophycocyanin
APCs	Antigen-presenting Cells
AR	Allosteric region
Arg	Arginine
Asn	Asparagine
BBB	Blood-brain barrier
BCRs	B cell receptors
BSA	Bovine Serum Albumin
Caco-2	Human Colorectal Adenocarcinoma
CDG	Congenital Disorders of Glycosylation
CMP-sialic acid	Cytidine-5-monophosphate-*N*-acetylneuraminic acid
CNS	Central Nervous System
CRD	Carbohydrate Recognition Domain
CTLs	C-type lectins
CYP	Cytochrome
DAMPs	Danger Associated Molecular Patterns
DCCM-1	High protein serum-free medium
DCs	Dendritic Cells
DC-SIGN	Dendritic cell-specific intercellular adhesion molecule-3-grabbing non-integrin
DMEM	Dulbecco's Modified Eagle Medium
DMRV	Distal Myopathy with Rimmed Vacuoles

EDTA	Trypsin-ethylenediaminetetraacetic Acid
ER	Endoplasmic Reticulum
FBS	Fetal Bovine Serum
FITC	Fluorescein isothiocyanate
Fu	Fraction unbound
GalNAc	*N*-acetylgalactosamine
GalNAcTs	*N*-acetylgalactosaminyltransferases
GI	Gastrointestinal
GlcNAc	*N*-acetylglucosamine
GNEM	GNE Myopathy
HEK	Human Embryonic Kidney
HepG2	Human Hepatoblastoma
hERG	human Ether-a-go-go-related
HIBM	Hereditary Inclusion Body Myopathy
IFN	Interferon
Ig	Immunoglobulin
IL	Interleukin
ITAM	Immunoreceptor Tyrosine-Based Activation Motif
ITIM	Immunoreceptor Tyrosine-Based Inhibitory Motif
IVIG	Intravenous Immunoglobulin
KI	Knock-in
KO	Knock-out
log BB	Blood-Brain Barrier Membrane Permeability
LogP	Octanol-water Partition Coefficient
ManNAc	*N*-Acetyl-D-mannosamine
ManNAc kinase	*N*-acetylmannosamine kinase
ManNAc-6-P	*N*-Acetyl-D-mannosamine-6-phosphate

MFI	Mean Fluorescent Intensity
MHC	Major Histocompatibility Complex
NCAM	Neural Cell Adhesion Molecule
NES	Nuclear Export Signal
Neu5Ac	*N*-acetylneuraminic acid
NK	Natural Killer
OCT2	Organic Cation Transporter 2
PAMPs	Pathogen Associated Molecular Patterns
Papp	Apparent Permeability Coefficient
PEP	Phosphoenolpyruvate
PFA	Paraformaldehyde
P-gp	P-glycoprotein
PMM2-CDG	Phosphomannomutase 2- Congenital Disorders of Glycosylation
PNA	Peanut agglutinin
Pro	Proline
PRRs	Pattern Recognition Receptors
Ser	Serine
Siglec	Sialic acid biding immunoglobulin-like lectins
SNA	*Sambucus nigra* agglutinin
TCRs	T cell receptors
Thr	Threonine
TLRs	Toll-like Receptors
TMB	3,3',5,5'-Tetramethylbenzidine
TPSA	Topological Polar Surface Area
Tyr	Tyrosine
UDP-GlcNAc 2-epimerase	UDP-*N*-acetylglucosamine 2-epimerase

UF	Unknown Function
VDss	Distribution Volume
WT	Wild Type

1 | Introduction

1.1 Glycosylation

Glycosylation is one of the most relevant post-translational modifications processes, where carbohydrates are enzymatically attached to an acceptor molecule, commonly proteins or lipids, through glycosidic linkages.[1] Glycosylation process is found in almost all known living organisms, including eukaryotes, eubacteria and archaea.[2,3] Glycosylation in eukaryotes, occurs predominantly along the secretory pathway beginning in the endoplasmic reticulum (ER) and being completed in the Golgi complex and is orchestrated by glycosyltransferases and glycosidases.[4,5]

Regarding protein glycosylation, the two main types documented are N-glycosylation and O-glycosylation (**Figure 1**).[6] N-glycosylation is characterised by the addition of glycans to specific asparagine (Asn) residues. N-glycosylation biosynthesis is initiated in the ER, where a precursor oligosaccharide is assembled on a resident lipid carrier, dolichol pyrophosphate.[4,7] After the biosynthesis of this precursor, ER transmembrane glycosyltransferases transfer the glycan portion from the dolichol pyrophosphate to a protein *via* a N-glycosidic linkage of a *N*-acetylglucosamine (GlcNAc) to an Asn residue. This Asn residue must be comprised on the consensus amino acid sequence Asn-X-serine (Ser)/threonine (Thr) in which "X" stands for any amino acid except proline (Pro).[8] The second stage of N-glycosylation includes the hydrolytic removal of monosaccharides ("trimming") and the re-glycosylation with other monosaccharides ("processing") in the ER and then in the Golgi.[9] These sugar additions convert a limited repertoire of N-glycans into a vast array of mature and complex N-glycans.[8]

O-glycosylation, on the other hand, results from the attachment of glycans to the hydroxyl group of a Ser, a Thr, and, less often, tyrosine (Tyr) or other side chains with hydroxyl residues. O-glycosylation is usually initiated in the Golgi by *N*-acetylgalactosaminyltransferases (GalNAcTs) that transfers *N*-acetylgalactosamine (GalNAc) residue to the hydroxyl group of a Ser or Thr residue in the protein. Subsequently, this Ser/Thr-GalNac structure go through sequential enzymatic elongation steps to form longer and more complex structures.[5] With a few exceptions, O-glycans are small and non-processed structures, being generated by single sugar transfers and not by the transfer of any pre-assembled precursors as in the case of N-glycans.[5]

Both processes of glycosylation described above can be further modified by sialylation, sulfation, acetylation, fucosylation, and polylactosamine-extension, introducing considerable variety to the proteome.

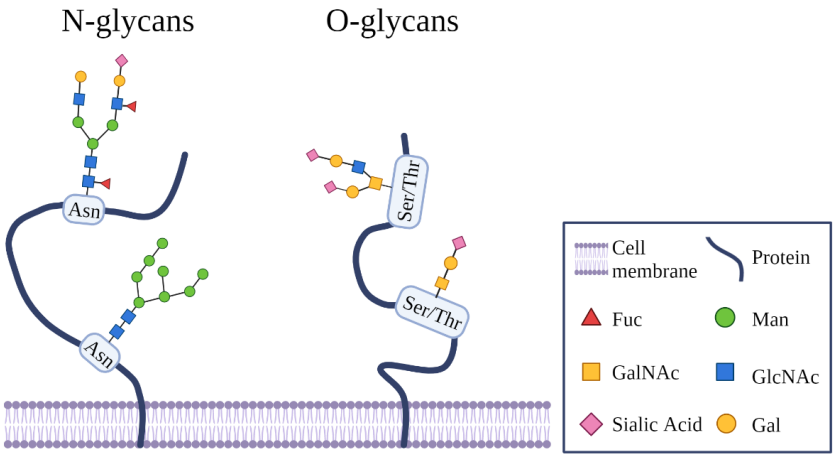

Figure 1 – Comparison of N-glycans and O-glycans decorating proteins at cell surface. N-glycans are linked to the nitrogen atom of asparagine (Asn) whereas O-glycans are attached via O-linkage to serine (Ser)/ threonine (Thr). Fucose (Fuc), mannose (Man), galactose (Gal), *N*-acetylgalactosamine (GalNAc), *N*-acetylglucosamine (GlcNAc).

1.1.1 The Biological Role of Glycosylation

Glycosylation has been shown to be essential in several biological activities, including cell adhesion, cellular interactions, and signalling, which are fundamental to the normal development, growth and differentiation of cells and tissues.[10]

At the protein level, glycosylation affects protein folding, solubility, activity, stability, and subcellular targeting. Protein glycosylation is crucial for the correct formation of protein complexes and higher-order protein structures, mainly due to the modulation of protein-protein interactions.[6] At a higher level, glycosylation is important for cell-cell and cell-matrix recognition. Glycans lining the cell surface serve as docking sites for cell-cell and extracellular communication, immune recognition, pathogen attachment and biological signalling.[11] The huge diversity of glycans, due to different positions of a given saccharide and stereochemistry options, contributes to the high specificity of the processes and interactions outlined above.[6]

However, deregulation of glycosylation pathways can cause critical alterations of physiological processes and is commonly found to modulate the course of various malignancies and pathological pathways such as inflammation.[12] Aberrant glycosylation is often observed in cancer and related to tumour aggressiveness and to poor clinical outcome.[11]

1.2 Glycosylation and Immune Response

Glycosylation has a crucial role in the immune function, since the majority of the molecules involved in the immune response are glycoproteins[13] and most of the microbial patterns are glycans or glycoconjugates.[14] Furthermore, lectins or glycan-binding proteins, such as galectins or sialic-acid binding immunoglobulin-like lectins (Siglecs), are responsible for modulating most of the immune response. The main mechanisms of the immune response and the importance of glycosylation for the assembly of an adequate immune response will be explored in the following sections.

1.2.1 Immune System

The immune system consists of a complex network of components and structures throughout the body, responsible for conferring protection against foreign bodies or cell changes. The immune system must be able to distinguish these differences, discriminating host molecules ("self") from foreign ("non-self") and harmless non-self from unsafe non-self.[15] There are two main types of immune response: the innate and the acquired response.

The innate immune response develops earlier and is characterized by the lack of immunologic memory, remaining unchanged regardless of the number of encounters with the same antigen.[16] The innate immunity comprises different defence mechanisms as biological barriers, phagocytic cells (neutrophils, macrophages), antigen-presenting cells (APCs) (dendritic cells (DCs)), cytotoxic cells (natural killer (NK) cells) and molecules such as complement proteins. The cells involved in the innate immune response recognize pathogen associated molecular patterns (PAMPs) and danger associated molecular patterns (DAMPs)[17] by interaction with pattern recognition receptors (PRRs), including the toll-like receptors (TLRs). After recognition of these patterns, several signal transduction pathways are activated resulting in the secretion of cytokines among other factors. Cytokines, as interleukin (IL)-6 and IL-1β, promote the recruitment and activation of immune cells, promoting phagocytosis, neutralisation, and clearance of pathogens.[18] The innate immune response, through the antigen presentation and cytokine expression, has a crucial role in the activation of the acquired immunity.

The acquired response is typically slower than the innate immune response. But acquired immunity is antigen specific and provides long-lasting protection due to the development of immunological memory.[19] The principal cells involved in the acquired response are lymphocytes that have specific receptors capable of distinguish similar antigens.

Cell-mediated immunity is carried out by T cells, which are activated after antigen presentation through specialised molecules, such as major histocompatibility complex (MHC). There are two pathways in which antigen peptides can become available for presentation, the cytosolic and the endocytic pathway.[20] The cytosolic pathway comprehends the proteolysis of cytosolic proteins by the proteasome. Then, the peptides are transported to the ER where they are loaded to an MHC class I (MHC-I) molecule, which is expressed by all nucleated cells. The peptide is exposed at the cell surface connected to MHC-I and can be presented to cytotoxic T cells, leading to its activation.[20] Whereas the endocytic pathway comprises antigen processing from internalised proteins. These proteins are processed and loaded into MHC class II (MHC-II) molecules, only expressed in APCs. The peptide-MHC complex is transported to the cell surface and detected by helper T cells.[20] Helper T cells mediate the activation and proliferation of other immune cells through cytokine secretion. Nevertheless, antigen recognition alone is not sufficient for the proper activation of T cells. The presence of co-stimulatory molecules, like CD80 and CD86 molecules expressed on APCs, and cytokines is required.[21]

On the other hand, to initiate humoral immunity, mediated by antibody molecules, each naïve B cell recognizes a specific antigen and is activated and differentiated into plasma B cells. Plasma cells are responsible for the secretion of antibodies with high specificity to the antigen, leading to antigen neutralisation and elimination.[22]

1.2.2 Glycosylation in the Innate Immune System

Glycosylation, directly or indirectly, plays several roles in immune function. For instance, glycosylation is crucial for microbe-host interactions, facilitating the binding or reducing the attachment of the pathogen.[6,14] An example of the first case is the infection with the enteropathogenic *Escherichia coli* (*E. coli*), where colonization is mediated by P pili, a bacterial fibrillae composed by a glycan-binding subunit that specifically recognizes galactose-β1,4-D-galactose disaccharide epitope found on the surface of epithelial cells,[23] promoting *E. coli* adherence. On the other hand, glycans can prevent the microbial attachment and invasion by for instance, reinforcing the physical barriers that are part of the innate immune response. Mucins are high molecular-weight glycoproteins, with extensive O-glycosylation. O-glycans bind water molecules and form a viscous barrier between the epithelial cells and the microorganisms.[24,25]

As referred in the previous section, the innate immune system functions through the recognition of molecular “patterns”, that commonly contain or are exclusively glycans. The recognition of certain glycans by the PRRs is enough to initiate signalization pathways and set an immune response. Moreover, glycans have a direct impact on the structure of PRRs by affecting folding,

multimerization, trafficking, cell-surface stability, and degradation.[14] For instance, TLRs are heavily glycosylated, and it has already been demonstrated that these glycans are crucial for TLR function. TLR variants with glycan site mutations failed to activate the signalling pathways upon ligand binding.[26]

1.2.3 Glycosylation in the Acquired Immune System

The acquired immune response is no less affected by glycosylation. In fact, several glycans are epitopes recognized by T cell receptors (TCRs) or B cell receptors (BCRs). The most well-known example is the ABO(H) blood group system.[27] These are glycans or glycolipids on the erythrocyte membrane. Individuals with a certain group of glycans recognize them as "self" and produce antibodies against the other group of glycans. When in contact with cells from another blood group, the antibodies will bind and coat the erythrocyte leading to cell lysis, revealing the potent antigenic power of glycans in the acquired immune response.[14]

In addition, glycosylation also alters TCRs and BCRs activities, modulating interactions of receptors and ligands, thereby altering receptor endocytosis, clustering, and signalling.[28] Actually, lower complexity of N-glycosylation on TCR results in increased TCR clustering and signalling even in the presence of a lower amount of antigen.[14] Effects of glycans on antibodies have also been demonstrated to affect attachment and signalling through immune cell receptors, and evidence suggests that it may be linked to antigen specificity and affinity maturation of antibodies.[29]

1.2.4 Glycan-binding Proteins

Three receptor families that are involved in glycan recognition – C-type lectins (CTLs), galectins and Siglecs – constitute another major component of the immune system involved in either the innate or acquired responses. All these proteins contain at least one carbohydrate recognition domain (CRD).[30]

The Siglecs are cell surface receptors that recognize sialic acid residues (**Figure 2**). Siglecs are commonly expressed on the surface of immune cells, such as DCs, macrophages, monocytes, neutrophils, and B cells.[30] These proteins aside from having the capacity to bind sialic acids present in other cells (in *trans*) can also bind to sialic acid residues present in the same cell (in *cis*). The majority of Siglecs are responsible for inhibitory signalling, and almost all Siglecs have an immunoreceptor tyrosine-based inhibitory motif (ITIM) on the cytoplasmic tail or associated with ITIM-containing receptors to regulate the response of an immune cell upon encountering a

"self" sialic acid.[28] Some Siglecs can also interact with DAP12, a transmembrane protein that contains immunoreceptor tyrosine-based activation motifs (ITAMs) resulting in signal transduction.[31] In addition, there are Siglecs that do not interact with either ITIMs or ITAMs, as Siglec-1 that is associated with phagocytosis of sialylated antigens.[32] Consequently, Siglecs can convey regulatory signals that differentially shape the immune cell response.[28]

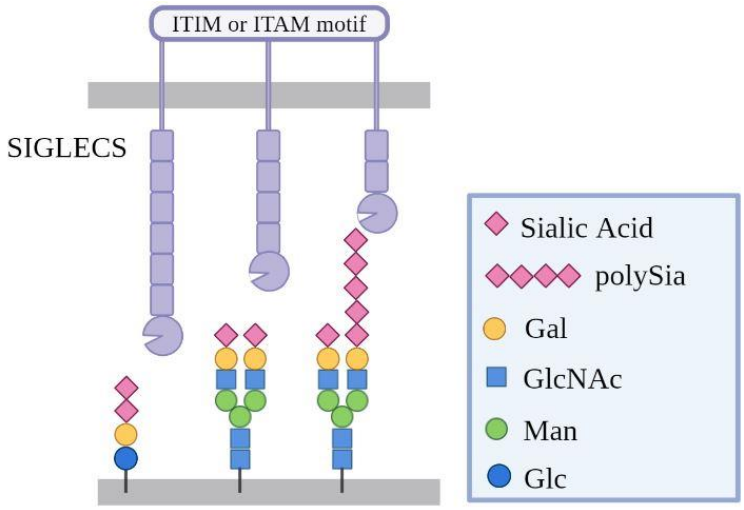

Figure 2 – Generic representation of sialic acid biding immunoglobulin-like lectins (Siglec) receptors. Siglecs recognize sialic acid-containing glycans and polysialic acid (polySia). Immunoreceptor tyrosine-based inhibitory motif (ITIM), immunoreceptor tyrosine-based activation motif (ITAM), galactose (Gal), *N*-acetylglucosamine (GlcNAc), mannose (Man), glucose (Glc).

Galectins are commonly secreted and defined by a conserved CRD that recognizes *β*-galactosides.[33] In the immune response galectins are usually expressed by activated not resting lymphocytes and overexpressed in activated macrophages and in regulatory T cells (a subset of T cells). The expression of galectins in these cells is modulated by different inflammatory stimuli dependent on the activation state of the cells.[34,35] Nowadays, it is assumed that galectins play a crucial role in the regulation of immunity and inflammation and can modulate cancer progression.[33,36,37]

CTL receptors are membrane-bound calcium-dependent carbohydrate-binding proteins.[38] CTLs can be divided into two types: the mannose-specific CTLs that contains an amino acid motif specific for mannose and/or fucose terminated glycans and the galactose-specific CTLs with a distinct amino acid motif in the CRD and that have specificity for galactose-terminated or GalNAc-terminated glycan structures.[30,38] Often CTLs are PRRs, such as Dectin-1, collectins and dendritic cell-specific intercellular adhesion molecule-3-grabbing non-integrin (DC-SIGN), so these lectins are important for pattern recognition. CTLs also have other roles in the immune response, such as promoting leukocyte function, migration, antigen uptake, signalling, and cell adhesion.[14]

1.3 Congenital Disorders of Glycosylation

Changes in glycosylation are a common feature in several disease scenarios, resulting from the dysregulation of the glycan biosynthetic pathway in response to certain stimuli like inflammation, infection, or oncogenic alteration, or have a defect in innate metabolism, such as in the case of congenital disorders of glycosylation (CDG).[11]

CDG comprise a heterogeneous group of more than 150 diseases[39] caused by mutations that affect different steps along the glycosylation pathways, resulting in hyper- or hypo-glycosylation of glycoconjugates. Nowadays, CDGs are classified into four groups: N-glycosylation-related, O-glycosylation-related, lipid and glycosylphosphatidylinositol biosynthesis defects and, lastly, conditions that have multiple glycosylation pathways affected.[40]

The majority of CDGs are monogenic diseases inherited in an autosomal recessive manner.[40] The phenotypic manifestations of these CDGs are usually multi-systemic, mainly affecting the central nervous system, as well as the gastrointestinal, hepatic, and immune systems, due to the wide range of glycan functions in different organs and tissues.[39,41]

Given the broad spectrum of clinical manifestations and genetic etiology of CDGs, clinical diagnosis is challenging and relies on molecular testing. The recent arrival of next-generation sequencing has rapidly expanded both the discovery of new CDGs and the unravelling of many unsolved diagnosis cases.[42] In fact, it is assumed that lots of individuals with CDGs are misdiagnosed, so the incidence and prevalence of all types of CDGs are not well-established, but based on population allele frequencies the expected birth prevalence of the most common CDG, phosphomannomutase 2-CDG (PMM2-CDG), could be as high as 1:20 000.[43,44]

CDGs treatment options available are limited, mostly relying on symptomatic and preventive approaches. Only a few CDGs curative therapies are being used, and those include monosaccharide supplementation and organ transplantation.[45]

1.4 GNE Myopathy

GNE myopathy (GNEM) is an ultra-rare CDG which affects 1 to 9:1 000 000 individuals worldwide (Orphanet; https://www.orpha.net/). GNEM was reported for the first time in Japan and recognized as distal myopathy with rimmed vacuoles (DMRV)[46] and in Israel as hereditary inclusion body myopathy (HIBM).[47] Other names such as Nonaka myopathy, inclusion body myopathy 2 and quadriceps-sparing myopathy have emerged since then. In 2001, mutations in

the *GNE* (9p13.3), the gene encoding the bifunctional enzyme UDP-*N*-acetylglucosamine 2-epimerase (UDP-GlcNAc 2-epimerase)/*N*-acetylmannosamine kinase (ManNAc kinase) were identified[48] as the cause of the disease and confirmed that all these myopathies were indeed the same pathological condition.[49] Since then, and to avoid confusion due to the different historical names it was agreed to unify them into a single disease entity known as GNE myopathy.[50]

1.4.1 Clinical Presentation

Patients with GNEM typically present manifestations in early adulthood, between 20 and 40 years of age[51]. The usual clinical symptoms are anterior tibialis weakness, gait disturbance, incapacity to lift the toes and foot drop. This clinical presentation of GNEM is the result of progressive skeletal muscle atrophy: it progresses from the distal to proximal skeletal muscles of the lower extremities followed by upper extremities and sparing of the quadriceps.[51] Disease progression may lead to complete loss of skeletal muscle and result in dependence of caregivers and use of a wheelchair.[52]

Muscle cells from GNEM patients show small angular fibres and the presence of rimmed vacuoles.[53] The rimmed vacuoles can especially be found in atrophic fibres and may be absent in unaffected muscles. Most of the GNEM patients retain quadriceps sparing through several decades, while only a minority (~5%) have quadriceps weakness early on.[54] Accordingly, it is recommended to avoid biopsy of the quadriceps muscles for research of rimmed vacuoles in the tissue. Aside from the muscle weakness and atrophies, the neurological examination is typically normal. Therefore, GNEM is not associated with cognitive impairment,[55] in contrast to most CDGs.

1.4.2 Genetics and Genotype-phenotype Correlations

GNEM is an autosomal recessive inherited disease, which means that GNEM patients have pathogenic variants in both *GNE* alleles. Patients may be homozygous for a single mutation or compound heterozygous for two distinct mutations in either the same or different domains of the enzyme. Remarkably, no patients have been identified with two null mutations (nonsense or frameshift mutations), suggesting that absent GNE activity is incompatible with life.[56,57]

There are already more than 200 *GNE* causing mutations identified and the spectrum of mutations is constantly growing.[58] Some mutations have been defined as ethnic founder mutations found in Middle Eastern (p.M743T),[59] Japanese (p.C44S, p.D207V, and p.V603L),[60] Roma Bulgarian (p.I618T)[61] and Indian/Asian populations (pA.662V and V727M)[62,63] (**Figure 3**). The large

majority of pathogenic variants associated with GNEM are missense mutations, but other mutations such as nonsense mutations, insertions, deletions, intronic and splice site mutations have also been described.[58,64]

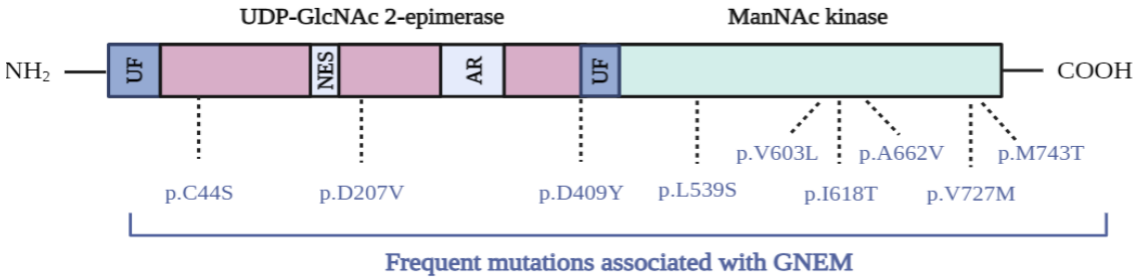

Figure 3 – GNE protein structure and location of frequent GNE mutations. The structure of the hGNE2 variant has two main domains the UDP-GlcNAc 2-epimerase enzymatic (in red) and the ManNAc kinase enzymatic domain (in green). Both includes a domain of unknown function (UF). Putative nuclear export signal (NES); experimental allosteric region (AR) for binding of CMP-sialic acid. Based on Carrillo, N. *et al* (2018).[65]

Genotype-phenotype studies showed considerable variability in disease severity, suggesting that certain point mutations are linked to age at onset, symptoms, severity, and speed of the disease progression. Cohort-based studies suggest that patients with one of the most common mutations in Japan p. A207V are predisposed to later onset of symptoms and milder phenotype than patients with the p.V603L variant and phenotypic differences between homozygous and compound heterozygous carriers were also reported.[66] Furthermore, patients with one mutation in each enzymatic domain had the lowest proportion of ambulant patients, earliest onset and the earliest use of wheelchair compared to patients with both mutations within the epimerase or kinase domain.[51]

However, genotype-phenotype correlation studies in patients homozygous for one mutation have shown significant phenotype variability even between families, suggesting that the type of the *GNE* mutation only partially contributes to the severity of the disease.[51,67] A recent systematic review of all cohort studies to date report that *GNE* genotype only explains 20% of phenotypic variability.[68] Additionally, some asymptomatic cases with confirmed causative mutations have been reported, indicating an incomplete penetrance of the disease or the existence of other factors that can mitigate the symptoms.[55]

Understandably, a common problem of these cohort studies with an ultra-rare disease like GNEM is the lack of statistical significance. Therefore, a reliable correlation between genotype-phenotype remains to be fully elucidated.[55]

1.4.3 Proposed Molecular Mechanisms

The *GNE* gene encodes for UDP-GlcNAc 2-epimerase/ManNAc kinase that initiates and regulates the synthesis of sialic acids, a group of derivatives of neuraminic acid. Sialic acids are terminal monosaccharides of most glycans found on proteins and cell surfaces, where they mediate different biological functions.[69] The most abundant sialic acid in humans and precursor of other sialic acids is *N*-acetylneuraminic acid (Neu5Ac).[70]

1.4.3.1 Sialic Acid Biosynthesis

The biosynthesis of Neu5Ac (**Figure 4**) is an intracellular pathway initiated by the conversion of GlcNAc into *N*-Acetyl-D-mannosamine (ManNAc) by UDP-GlcNAc 2-epimerase, followed by phosphorylation of ManNAc into ManNAc-6-P by ManNAc kinase.[71] Subsequently, sialic acid synthase converts ManNac-6-P to Neu5Ac-9-P in a condensation reaction with phosphoenolpyruvate (PEP), after which Neu5Ac-9-P is dephosphorylated to Neu5Ac. In the nucleus, Neu5Ac is activated into cytidine-5-monophosphate-*N*-acetylneuraminic acid (CMP-sialic acid),[72] which is transported into the Golgi where it can be incorporated into glycoproteins and glycolipids by sialyltransferases.

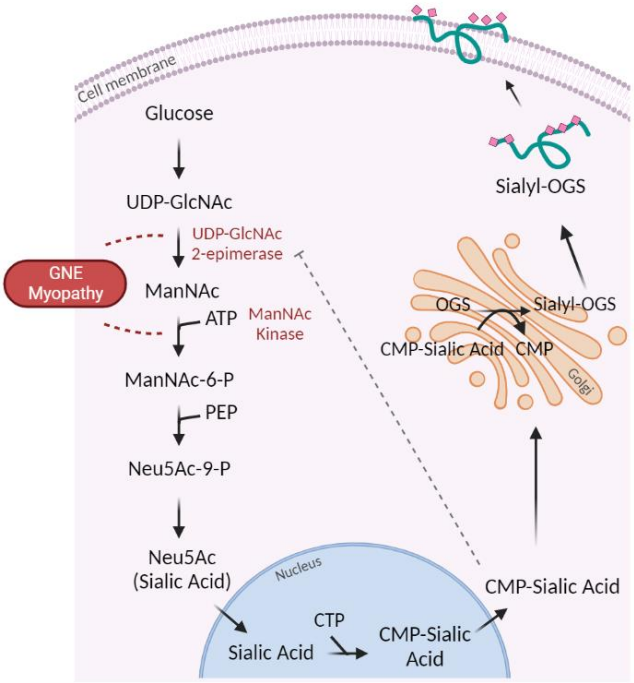

Figure 4 – Sialic acid biosynthesis. The biosynthesis of sialic acid (Neu5Ac) occurs in the cytoplasm. The initial substrate is UDP-*N*-acetylglucosamine (UDP-GlcNAc), which derives from glucose. The bifunctional enzyme UDP-GlcNac 2-epimerase/ ManNAc kinase, encoded by *GNE* gene, catalyses the rate-limiting steps of Neu5Ac biosynthesis. Neu5Ac becomes activated by cystidine monophosphate (CMP)-sialic acid synthase in the cell nucleus. CMP-sialic acid is used as a donor of sialic acid in the Golgi apparatus for the generation of glycoconjugates. CMP-sialic acid also acts as cytoplasmic feedback inhibitor of the UDP-GlcNAc 2-epimerase enzyme by binding to its allosteric site. Phosphoenolpyruvate (PEP); cytidine triphosphate (CTP); oligosaccharides (OGS).

This pathway is regulated through feedback inhibition of UDP-GlcNAc 2-epimerase enzyme *via* binding of cytoplasmic CMP-sialic acid to its allosteric site.[65]

1.4.3.2 Hyposialylation and Alternative Pathomechanisms

Sialylation, as the end-product of sialic acid biosynthesis, is critical for several biological processes including cell adhesion, cellular interactions, and signalling.[69] *GNE* mutations presumably affect glycans sialylation since they affect the activity of UDP-GlcNAc 2-epimerase/ManNAc kinase, the rate limiting enzyme in the sialic acid pathway.

There are some clues suggesting that hyposialylation of muscle cell surface glycans play a significant role in GNEM pathogenesis, for example specific skeletal muscle glycans including α-dystroglycan, neural cell adhesion molecule (NCAM), neprilysin, GM3 ganglioside, and O-linked glycans have been reported to be hyposialylated in GNEM.[65,73,74]

Although hyposialylation is typically assumed as the main cause of GNEM, several pieces of evidence suggest that the GNEM pathomechanism is more complicated and may not be exclusively linked to the impaired sialic acid pathway. Firstly, GNE enzymatic activity is only partially reduced in patients (30-60% reduction) and this range of reduction is not expected to cause phenotype in classical metabolic myopathies.[54] In addition, the screening of muscle sialylation showed that it is only slightly reduced in some patients. Secondly, results from a phase 3 randomised, double-blind placebo-controlled trial with an extended formulation of Neu5Ac in GNEM patients failed to detect clinical efficacy not supporting hyposialylation as the main cause of disease.[75] Lastly, research laboratories have attempted to determine other unknown functions of GNE that could be part of the pathomechanism of this myopathy.

A deregulated ER-stress response has been identified as a source of muscular damage in GNEM,[76] and oxidative stress has also been acknowledged to be involved, not as consequence of tissue injury, but rather as an upstream phenomenon to muscle atrophy.[77] In fact, skeletal muscle tissue demands extensive and continuous energy supply, as well as an adaptation to changes in metabolism and oxygen consumption to fulfil its primary functions. Therefore, it is evident a prone vulnerability of the muscle to a dysregulation of the cellular stress response.

Although immune-mediated response and inflammatory changes are not common manifestations in GNEM,[65] inflammation can also be at the root of the earliest stages of the disease, as it has been implicated in many other metabolic disorders.[78] Inflammatory cell infiltration with increased expression of MHC-I is occasionally reported in muscle biopsies of early stage GNEM

patients.[79,80] Moreover, our group has previously shown that sialic acid shortage leads to increased cell surface expression of the MHC-I.[81,82]

Despite these advances, it remains unclear the process by which a *GNE* mutation leads to muscle disease and the functional implications of MHC-I and other cell stress.

1.4.4 GNE Myopathy Models

In the past decades, cell lines with *GNE* mutations or decreased *GNE* expression have been used for studying disease pathomechanisms or new therapeutic strategies.[83] These cell models are extremely important as reports of patients reveal a large degree of uncertainty and because of the low availability of patient-derived cells. Despite the usefulness of these *in vitro* models for characterization of the GNE protein, evaluation of pathogenicity of newly identified *GNE* mutations or to study cellular modifications, animal experiments remain essential to understand the mechanisms underlying GNEM and to discover and approve new diagnose and treatment methods.

There are three mouse models of GNEM currently available to facilitate the understanding of disease pathophysiology and identification of potential therapies. A complete knock-out (KO) mouse model of the *Gne* gene is no compatible with life and displays early embryonic lethality.[56] Therefore, the models available are *Gne*-deficient mice, but they fail to mimic the GNEM phenotype observed in the patients, which limits their pre-clinical potential.

The first *Gne* knock-in (KI) mouse model was created by homologous recombination strategy, introducing the Middle Eastern founder mutation p.M743T in the kinase domain.[84] Unexpectedly, this mouse model showed high mortality rate in the first generation due to renal damage, characterized by severe glomerular disease,[84,85] which is not typically observed in GNEM patients. However, the importance of sialic acid to the kidney and protein glycosylation patterns may differ between species. Apart from the kidney phenotype, the mice that overcome the renal damage fail to present any muscle phenotype.[86]

A transgenic mouse that expressed the human *GNE* p.D207V mutation (one of the most prevalent mutations among Japanese GNEM patients) was the first mouse model generated that resembles the clinical, pathological, and biochemical features of the disease.[87] The *Gne*$^{(-/-)}$h*GNE*D207V-Tg mice exhibit late onset progressive muscle atrophy and pathological markers, including the presence of rimmed vacuoles in atrophic fibres. Interestingly, this model exhibits marked hyposialylation in serum, muscle, and other organs, highlighting the potential key-role of

hyposialylation in GNEM mechanism.[87] Another transgenic mouse model, the *Gne*$^{(-/-)}$h*GNE*V603L-Tg, which expresses the most prevalent *GNE* mutation in Japanese patients (p.V603L) was generated.[88] In this mice hyposialylation in serum, muscle and other organs, such as kidney, was also observed. It also exhibited late onset myopathy with reduction in motor performance seen from 30 weeks. Nevertheless, this mouse model also showed renal pathology due to hyposialylation.[89]

Overall, none of these models consistently recapitulate the GNEM phenotype observed in humans. The development of novel animal models is then crucial for understanding disease pathology and drug discovery. Nowadays, important attempts are being made towards new GNEM models in both mice and zebrafish.[90]

1.4.5 Therapeutic Options

Up to date, there is no approved treatment for GNEM. However, there are some efforts for developing improved therapeutic strategies based either on supplementation with sialic acid/sialic acid precursors or restoring GNE enzymatic activities by gene or cell therapy.

1.4.5.1 Supplementation therapy

Supplementation therapy is based on the hypothesis that if GNEM pathology is due to hyposialylation, increasing the sialic acid content may overcome it.[65] Highly sialylated glycoproteins, such as intravenous immunoglobulin (IVIG), and pathway substrates, including ManNAc and Neu5Ac, are examples of sialylation increasing therapies.

Since immunoglobulins G (IgG) contains 8 μmol of Neu5Ac/g, IVIG was infused in patients (ClinicalTrials.gov: NCT00195637). IVIG administration improved muscle strength and function but failed to increase the sialylation of target glycoproteins and there were no demonstrable histological changes.[91]

An extended-release formulation of Neu5Ac (Ace-ER) was developed and orally administrated to GNEM patients in a phase 2 randomized, double-blind, placebo-controlled trial (ClinicalTrials.gov NCT01517880). In this study patients receiving a higher dose of Ace-ER showed an improvement on upper extremity strength compared to the group receiving a lower dose, suggesting that the administration of Ace-ER to patients stabilized muscle strength.[92] Unexpectedly, phase 3 randomized, double-blind, placebo-controlled trial (ClinicalTrials.gov

NCT02377921) failed to demonstrate Ace-ER treatment benefits for muscle strength maintenance when compared to placebo, and this therapeutic strategy was set aside.[75]

ManNAc is the first sialic acid precursor affected in GNEM and is also a substrate of the kinase domain of the GNE enzyme. Although ManNAc do not overpass the second step catalyse by GNE, ManNAc overpasses the rate-limiting feedback inhibition enzymatic step catalyse by the epimerase domain and can be phosphorylated into ManNAc-6-P by other kinase enzymes (e.g., GlcNAc kinase).[93] Oral supplementation with ManNAc was already evaluated in a phase 1 randomised, placebo-controlled, double-blind, single-dose study[94] (ClinicalTrials.gov NCT01634750; IND No.78 091) and in a phase 2 open-label clinical trial (ClinicalTrials.gov NCT02346461) and showed long-term safety, biochemical efficacy consistent with the mechanism of action in the skeletal muscle and preliminary evidence of clinical efficacy.[95] ManNAc supplementation is now awaiting the start of a phase 2 randomized, placebo-controlled, double-blind, multi-center study (ClinicalTrials.gov NCT04231266) to evaluate clinical efficacy of ManNAc in subjects with GNEM.

These supplementation options still have some disadvantages, including the need of a high daily dose that is linked with many gastrointestinal adverse effects.[75,95]

1.4.5.2 Genetic Therapy

Gene therapy in GNEM aims at delivering an unaffected copy of the *GNE* gene to target skeletal muscle tissues and restore/prevent the loss of muscle strength and function. A supply of normal *GNE* gene is delivered into patient muscles to restore the sialic acid biosynthesis but also to restore the additional, however still largely unknown, functions of the GNE protein that are essential for normal physiology.[90]

The adeno-associated viruses 8 (AAV8) vector has shown to effectively deliver the *GNE* gene to healthy[96] and GNEM mouse model.[90] Moreover, the systemic injection of the rAAVrh74.MCK.GNE viral vector resulted in a long-term expression of human wild type (WT) GNE in the muscles and in the improvement of the mild phenotype of the GNEM mouse model.[90] The inexistence of a reliable mouse model to fully access the efficacy of this therapeutic approach together with the pre-existence of serum antibodies to AAV8 in 50% of GNEM patients[97] studied hinders its approval.

1.5 New Approaches to Fight GNEM: The ProDGNE Project

As previously described, there are no approved therapies for GNEM, and supplementation therapies have shown adverse effects and low absorption. "ProDGNE – Novel therapeutic approaches to target GNE myopathy" is a 3-year translational pre-clinical research project, funded by the European Joint Programme on Rare Diseases (EJPRD/0001/2020), which aims to develop prodrugs to treat GNEM, using the ProTide technology (**Figure 5**).

A prodrug is a substance that is inactive and must be converted by metabolic or physico-chemical transformation to be pharmacologically active.[98] Normally, prodrugs are generated to improve the absorption, distribution, metabolization, excretion and toxicity (ADMET) properties of a drug. ProTide technology uses phosphate masking groups to improve the drug-like properties of the compounds and an intracellular activation mechanism for enzyme-mediated release of a nucleoside monophosphate. Among many existing phosphate prodrug strategies, the ProTide approach has been applied with success to nucleosides, as evidenced by the development and approval of the currently marketed antiviral drug Sofosbuvir.[99] Our collaborators from the School of Pharmacy and Pharmaceutical Sciences, Cardiff University already have experience with this technology and have applied phosphoramidate chemistry to GlcNAc for the treatment of osteoarthritis and other musculoskeletal diseases.[100]

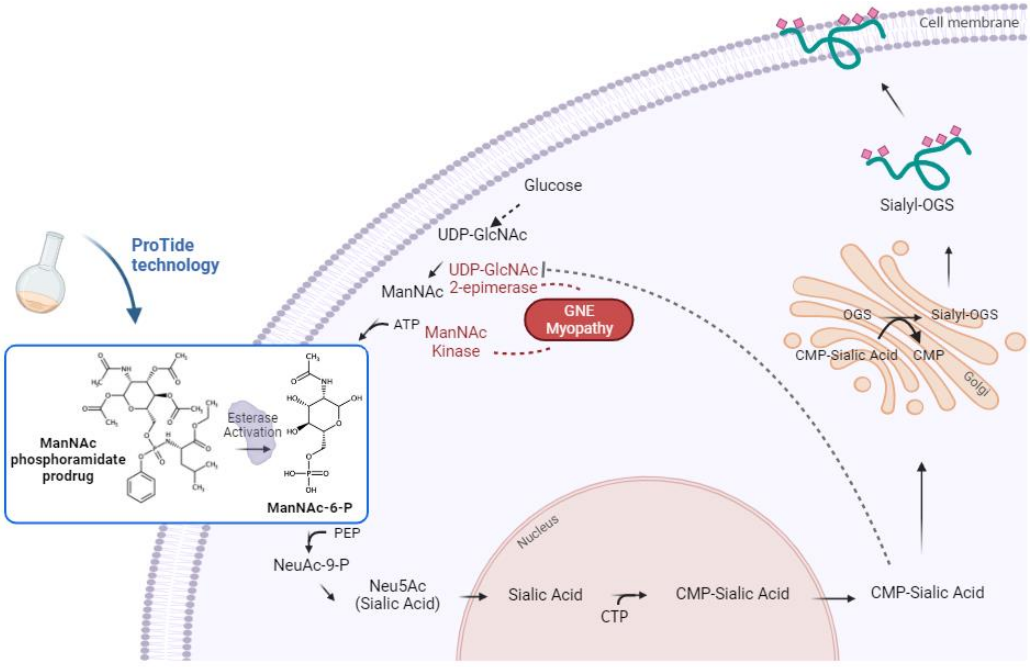

Figure 5 – The proposed mechanism of action of ProDGNE prodrugs in the sialic acid biosynthesis pathway. The ProTide is converted by esterase activation into ManNAc-6-P, the final product of the two steps catalysed by the GNE enzyme. Sialic acid (Neu5Ac); UDP-N-acetylglucosamine (UDP-GlcNAc); phosphoenolpyruvate (PEP); cytidine triphosphate (CTP); cystidine monophosphate (CMP); oligosaccharides (OGS).

Research is being conducted with the aim to improve the low permeability and plasma stability of ManNAc-6-P, the final product of the reactions catalysed by the GNE enzyme, using ProTide technology.[101] These prodrugs through the action of intracellular esterases will pass to its active form, the ManNAc-6-P (**Figure 5**). The delivery of ManNAc-6-P is thought to be more advantageous than the delivery of ManNAc, especially in patients who have mutations in the kinase domain.[101]

1.6 Objectives

The pathomechanism of GNEM is still not fully understood, and even though hyposialylation is assumed as the main cause of disease, evidence point to a far more complex pathomechanism for GNEM that may not be exclusively linked to an impaired sialic acid pathway.[76,102] In this dissertation one of our aims was then to explore alternative cellular and molecular mechanisms that may lead to this disorder, as means of identifying alternative therapeutic targets.

The importance of glycosylation, in particular sialylation, in the immune system[14,81] (previously discussed in subsection 1.2) has led us to hypothesize that the defective sialylation observed in GNEM influences the function of immune cells and consequently the immune response. During this thesis the immune response was evaluated by measuring the surface expression of molecular structures, such as MHC-I, and the production of inflammatory cytokines, such as IL-6. These immune response indicators were evaluated in a new cellular model of GNEM, the human embryonic kidney (HEK 293) cells with *GNE* KO, kindly provided by Prof. Rüdiger Horstkorte (Martin-Luther-Universität). Functional parameters, such as viability and metabolic activity, together with the syalophenotype of this new cell line were characterized to confirm whether it can be a good model to study GNEM.

This dissertation, developed within the framework of the ProDGNE project, had also the aim to help guide the selection of the new prodrugs developed by our partners in Cardiff University. In this line of investigation, the ADMET properties of the synthesized compounds were evaluated by computational analysis to select the compounds with best drug-like properties. Furthermore, assays to evaluate the toxicity and efficacy of the compounds in cell models were designed and optimized.

2 | Materials and Methods

2.1 Standards and Reagents

ManNAc and ManNAc-6-P were acquired from Biosynth Carbosynth® (Compton, UK). Dulbecco's Modified Eagle Medium (DMEM) with 4.5 g/L glucose supplemented with L-glutamine, and sodium pyruvate was obtained from Corning® (NY, USA). High protein serum-free medium (DCCM-1) was purchased from Sartorius (Beit Haemek, Israel). Heat inactivated fetal bovine serum (FBS), trypsin-ethylenediaminetetraacetic acid (EDTA) (0.05%), L-glutamine and Pen-Strep solution (Penicillin 10,000 units mL^{-1} and Streptomycin 10,000 µg mL^{-1}) were acquired from Gibco™ (Grand Island, NY, USA). Puromycin and Plasmocin® prophylactic were purchased from InvivoGen (San Diego, CA, USA). Trypan blue was acquired from NanoEntek (Guro-gu, Seoul, South Korea). Biotinylated *Sambucus nigra* agglutinin (SNA) was obtained from Vector Labs (Burlingame, CA, USA). Fluorescein isothiocyanate (FITC) conjugated peanut agglutinin (PNA), bovine serum albumin (BSA) and Tween20 were purchased from Sigma-Aldrich (St. Louis, MO, USA). Allophycocyanin (APC) conjugated Streptavidin was from BioLegend (San Diego, CA, USA). Polyclonal goat anti-mouse immunoglobulins/FITC goat F(ab')2 was purchased from Dako (Santa Clara, CA, USA). SiaFind™ α(2,6)-specific reagent kit biotinylated and SiaFind™ α(2,3)-specific kit biotinylated were acquired from Lectenz®Bio (Athens, GA, USA). Paraformaldehyde (PFA) was purchased from Polysciences Inc. (Warrington, PA, USA). FITC conjugated anti-HLA-ABC (W6/32) antibody, recombinant human interferon (IFN)-γ standard and human IL-6, IL-1β and IL-10 ELISA kits were from ImmunoTools GmbH (Friesoythe, Niedersachsen, Germany). 3,3',5,5'-Tetramethylbenzidine (TMB) single solution was acquired from Thermo Fisher Scientific (Waltham, MA, USA). Resazurin was obtained from Alfa Aesar (Thermo Fisher Scientific, Waltham, MA, USA).

HEK 293 cells were kindly provided by Prof. Rüdiger Horstkorte (Martin-Luther-Universität, Halle-Wittenberg, Germany). Human hepatoblastoma (HepG2) cell line was provided by Prof. Alexandra Fernandes (UCIBIO, Lisbon, Portugal). Mouse monoclonal IgG2a antibody 735 against polysialic acid was provided by Prof. Rita Gerardy Schahn (Medical School Hannover, Germany).

2.2 Cell Culture

HEK 293 wild type (HEK 293 WT), HEK 293 *GNE* knock-out (HEK 293 *GNE* KO) and HepG2 cells were cultured in DMEM 4.5 g/L glucose, supplemented with 10% FBS, 1% PenStrep, 1% L-glutamine and 3 μg/mL of Plasmocin® prophylactic to prevent mycoplasma contamination, in T75 culture flasks (Sarstedt, Nümbrecht, Germany) and incubated at 37 °C, with 5% CO_2 and a humidified atmosphere. HEK 293 *GNE* KO cells were generated by CRISPR/Cas9 technology (GLCNE CRISPR/Cas9 KO Plasmid (h): sc-406100 and GLCNE HDR Plasmid (h): sc-406100-HDR (Santa Cruz Biotechnology, Dallas, TX, USA)) and express a Red Fluorescent Protein (RFP) gene to visually confirm transfection and a puromycin resistance gene for selection of KO cells (see **Appendix 1**). HEK 293 *GNE* KO cells medium was supplemented with 2.5 μg/mL of puromycin to ensure KO selection.

At near-confluent stage, cells were detached with trypsin-EDTA (0.05%) for 5 min at 37 ºC. Afterwards cells were centrifuged at 200 *g* for 5 min (Eppendorf 5702R). Cell pellets were resuspended, and cell suspensions were used for cell splitting or sub-culture for the experiments described below.

2.3 Cell Viability and Metabolic Function

Resazurin assay is a simple, reliable, and sensitive method to measure cell viability. Cell growth creates a reduced environment capable of reducing resazurin (blue and non-fluorescent) to resorufin (red fluorescent dye). The colorimetric signal generated from the assay is proportional to the number of living cells (**Figure 6**).

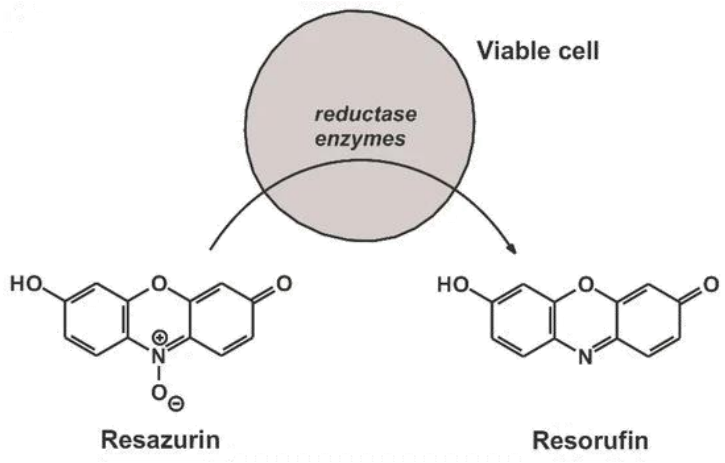

Figure 6 – The principle of resazurin cell viability assay. Reductases of viable cells reduce to resorufin. Chemical structures of resazurin and resorufin. Image from Csepregi, R. *et al.* (2018).[103]

Both HEK 293 WT, HEK 293 *GNE* KO and HepG2 cells were seeded in 96-well plates (3×10^4 cells per well) (Orange Scientific, Braine-l'Alleud, Belgium) in DMEM medium, in triplicate. Cells were allowed to attach for 24 h. To evaluate compound effect in cell viability, cells were exposed to ManNAc (100 µM) and ManNAc-6-P (100 µM) in DCCM-1 serum free medium for another 24 h (37 °C, 5% CO2).

After incubation, the medium was replaced by 200 µL of a 44 µM resazurin solution prepared in DCCM-1 medium. Cells were monitored during 4 h with absorbance reads on a SpectraMax 190 Microplate Reader at 570 nm and 600 nm at each 30 min, to determine the optimal incubation time for these cell lines and density. SoftMax Pro software (version 6.4.) was used to acquire data.

For measurement of cell viability and metabolic activity, unconverted resazurin background at 600 nm was discounted from resorufin absorbance at 570 nm. Three independent assays were performed.

2.4 Cell Surface Staining

HEK 293 WT and HEK 293 *GNE* KO cells were cultured in 6-well plates (6×10^5 cells/well) (Thermo Fisher Scientific) in DMEM medium and incubated at 37 ºC for 24 h to allow attachment. Cells were incubated with intermediates of the sialic acid biosynthesis, ManNAc (100 µM) and ManNAc-6-P (100 µM) in DCCM-1 serum free medium for 24 h at 37 °C, with 5% CO_2 and a humidified atmosphere.

Following exposure to ManNAc and ManNAc-6-P, cells were harvested and counted using an automatic cell counter (EVE™, NanoEntek) to have 1.5×10^5 cells per condition. Cells were washed with PBS 1× and centrifuged at 300 *g* for 5 min at 4 ºC (Eppendorf 5430 R).

SNA solution (1:100 in PBS + 1 % BSA), SiaFind™ α(2,3)-Specific solution (1:100 in PBS + 1 % BSA) and SiaFind™ α(2,6)-Specific solution (1:100 in PBS + 1% BSA) were added to cell pellets and incubated for 20 min at 4 ºC in the dark. Afterwards, fluorophore-labelled streptavidin (1:1000 in PBS + 1% BSA) was added and incubated for another 10 min at 4 °C.

Similar to the previous lectins, the 735 antibody against polysialic acid (1:100 in PBS + 1% BSA) was added to the cell pellets and incubated for 20 min at 4 ºC in the dark, after which the FITC conjugated goat anti-mouse immunoglobulins was added for 10 min at 4 ºC in the dark.

FITC-conjugated PNA solution (1:100 in PBS + 1% BSA) and MHC I antibody (2:100 in PBS + 1% BSA) were added to cell pellets and incubated for 30 min at 4 °C in the dark.

After each incubation, cell pellets were washed with PBS + 1% BSA and centrifuged at 300 *g* for 5 min at 4 ºC. Following the surface staining, HEK 293 WT and HEK 293 *GNE* KO cells were fixed with 300 µL of 2% PFA for flow cytometry analysis.

2.5 Flow Cytometry

Flow cytometry is a method used to count or/and distinguish different cell populations, and it is used for analysing the expression of cell surface and intracellular molecules as a result of fluorescent detection.

For each sample, at least 1×10^4 events corresponding to the relative size and granularity of HEK 293 cell line were acquired on an Attune Acoustic Focusing Cytometer (Applied Biosystems, Waltham, MA, USA). Data were analysed using FlowJo software version 10.0.5 (TreeStar, San Carlos, CA, USA) after cell gating and doublet exclusion by height and width parameters, to ensure only single cells were counted. *GNE* KO cells were gated in the HEK 293 *GNE* KO cell line using the RFP fluorescence to visually confirm transfection (**Figure 7**).

For each staining condition described in the previous section, the respective mean fluorescent intensity (MFI) of unstained control was subtracted and the results are presented as ΔMFI. At least three independent experiments were performed in duplicate.

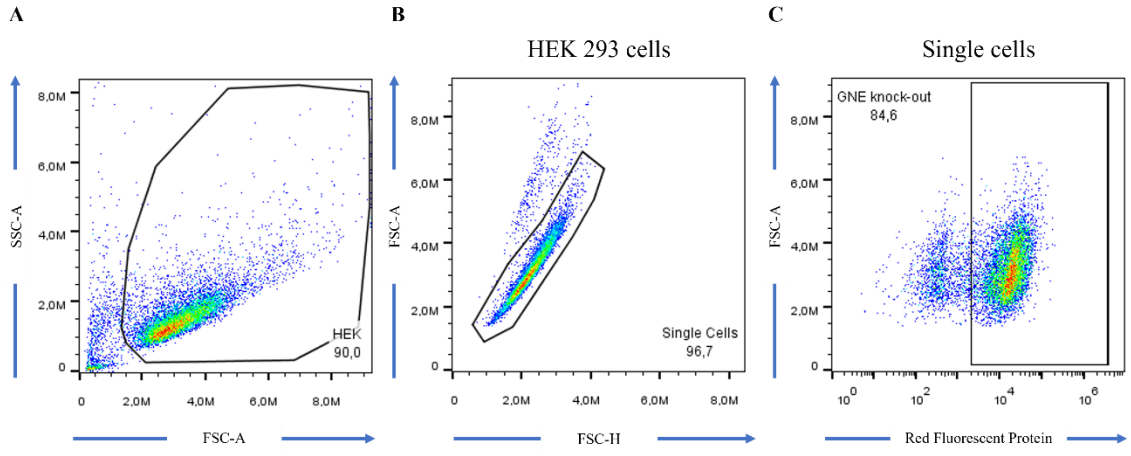

Figure 7 – Gating strategy of HEK 293 cell population and *GNE* KO cells. (A) Viable HEK 293 cells were gated from the dead cells and debris. **(B)** Single Cells gate avoid the quantification of doublets and other aggregated particles. **(C)** *GNE* KO cells with RFP fluorescence were selected in the HEK 293 *GNE* KO cell line.

2.6 Enzyme-linked immunosorbent assay (ELISA)

For ELISA assay, both HEK 293 cell lines were cultured in 6-well plates (6×10^5 cells/well) (Thermo Fisher Scientific) in DMEM medium and incubated at 37 ºC for 24 h. Cells were

incubated with ManNAc (100 μM) and ManNAc-6-P (100 μM) in DCCM-1 medium for 24 h and other subset of cells was incubated with IFNγ (100 μM) for 6 h at 37 °C, with 5% CO_2 and a humidified atmosphere. After incubation, the supernatant of each well was collected to quantify IL-6, IL-1β and IL-10 cytokines, using the human IL-6, IL-1β and IL-10 ELISA kit, respectively.

According to the kit instructions, 100 μL of diluted anti-human cytokine capture antibody (1:100 in PBS) were added to each well of a 96-wells ELISA plate (Costar) and incubated overnight at room temperature. After incubation, the capture antibody was removed and 300 μL of blocking buffer [PBS + 2% BSA (*w/v*) + 0.05% Tween20 (*v/v*)] were added to each well and incubated for 1h at room temperature. The blocking buffer was removed and 100 μL of serial dilutions prepared in blocking buffer (according to each cytokine kit detection range) and samples were added to the respective well in duplicate and incubated for 2 h at room temperature, followed by five washing steps.

Anti-human IL-6, IL-1β and IL-10 detection antibody was diluted 1:100 in blocking buffer and 100 μL of the diluted antibody were added to each well for another 2 h at room temperature, followed by five washing steps. Right after, 100 μL of Poly-Horseradish Peroxidase (HRP)-Streptavidin diluted in 1:1000 in blocking buffer were added to each well and incubated for 30 min at room temperature, and then the wells were washed. TMB substrate warm to room temperature was added to the wells (100 μL) and incubated for 1 h at room temperature in the dark.

After incubation, 50 μL of 2 M of sulfuric acid (H_2SO_4) were added to each well to stop the enzymatic reaction and the absorbance was read at 450 nm on a SpectraMax 190 Microplate Reader. SoftMax Pro software was used to collect the data. At least three independent experiments were performed in duplicate.

2.7 Statistical Analysis

All data was analysed using the Microsoft Office Excel and statistical analysis was performed using the GraphPad Prism 8.0 software (GraphPad Software, La Jolla, CA, USA) for Windows.

A Shapiro-Wilk normality test was employed to check the distribution of the data, and a Grubb's test to determine the presence of outliers. Two-tailed unpaired *t*-test was employed to assess statistical differences. Differences were considered statistically significant at the level of 0.05 ($p < 0.05$).

2.8 Prediction of ADMET-related endpoints by Computational Analysis

Prediction of ADMET properties of ManNAc, ManNAc-6-P, Sofosbuvir, and of the synthesized ManNAc phosphoramidate prodrugs (**1**–**12**) was carried out using the web server pkCSM (http://biosig.unimelb.edu.au/pkcsm/) from the Biosig Lab University of Melbourne.

To assess qualitatively the drug-likeliness of the synthesised compounds, chemical parameters, such as the octanol-water partition coefficient (LogP), and the topological polar surface area (TPSA) were retrieved from SwissADME software (ChemAxon).

3 | Results and Discussion

3.1 Characterization of a New Cell Model of GNEM

In the past decades, new cell models of GNEM have been developed either with *GNE* typical mutations or decreased *GNE* expression, but there is still a need of stable cell lines that are recognized by the scientific community as a good model for the study of GNEM mechanism, new diagnostic methods, and therapies.

In this work was used a new cell model of GNEM, the HEK 293 *GNE* KO cell line generated by CRISPR/Cas9 technology. It is important to highlight that in this cell line there is a KO of the *GNE* gene and, therefore, there is no expression of the GNE protein. So, there is a more drastic change than in patients because, as it was mentioned previously, no case in which the patient has two null mutations is known.[57] However, the use of such cellular model has the advantage of providing good result reliability and accuracy.

3.1.1 Sialophenotype of HEK 293 *GNE* KO cells

For characterization of the sialophenotype of the new GNEM cell model, the sialic acid profile in the cell surface of the HEK 293 WT and HEK 293 *GNE* KO was evaluated by lectin staining, using flow cytometry. HEK 293 cells were stained with lectins, such as SNA and PNA, and with SiaFind™ α(2,3)-specific and α(2,6)-specific solutions from Lectenz®Bio (**Figure 8**).

Commercially available lectins are an important tool in glycobiology for glycan content analysis, due to the ability of lectins to bind to specific carbohydrate structures.[104,105] SNA lectin, from the elderberry *Sambucus nigra*, predominantly recognizes terminal Neu5Ac in an α(2,6)-linkage with either galactose or with GalNAc in N-glycans. In turn, PNA lectin from peanut has specificity for the desialylated core 1 mucin type O-glycan, therefore a higher staining is associated to a lower content of Neu5Ac (see **Appendix 2**). Quantification of the sialic acid content at the cell surface using SNA and PNA lectins is a common method in muscle biopsies of GNEM patients.[106,107]

In this work, Lectenz®Bio reagents specific for Neu5Ac in an α(2,3)-linkage and in a α(2,6)-linkage (hereafter named as SiaFind α(2,3)-specific and SiaFind α(2,6)-specific) were also used. These solutions are novel recombinantly expressed proteins that may overcome the disadvantages of plant lectins, including high lot-to-lot variations and autoglycosylation,

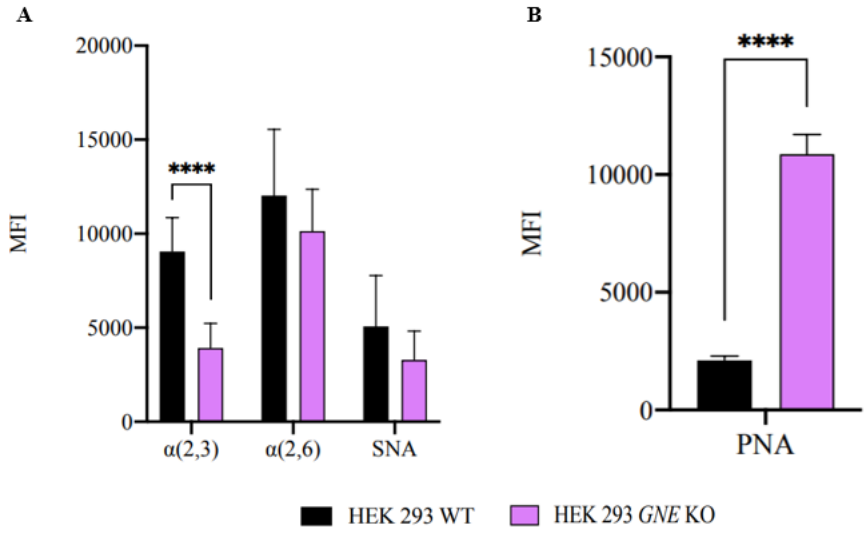

Figure 8 – Characterization of sialic acid profile by lectin staining. (**A**) SiaFind α(2,3)- and α(2,6)-specific staining solutions, and SNA staining of HEK 293 WT and HEK 293 GNE KO cells. (**B**) PNA staining of HEK 293 WT and HEK 293 GNE KO cells. For each condition at least 1×10^4 events corresponding to the relative size and granularity of HEK 293 cells were acquired on an Attune Acoustic Focusing Cytometer using the gating strategy depicted in Figure 7. Values represent MFI (mean ± SD). Significant differences at **$p < 0.01$, **** $p < 0.0001$ ($n \geq 3$).

Overall, a decrease in the staining of the HEK 293 *GNE* KO cells with SiaFind α(2,3)- and α(2,6)-specific solutions and SNA lectin was observed (**Figure 8A**), with a significant difference for the SiaFind α(2,3) staining ($p < 0.0001$). An MFI decrease with SNA and SiaFind α(2,6)-Specific solution was also observed but the difference between HEK 293 *GNE* KO and WT cells was not statistically significant ($p > 0.05$). Since both proteins recognize sialic acid in an α(2,6)-linkage, these results seem to indicate that the KO of the *GNE* gene affects more the sialylation in α(2,3) than in α(2,6). As far as we are aware, this effect has not been described in samples of GNEM patients. In fact, the difference between sialylation in α(2,3) and α(2,6) may be explained by the cells used in this work. Many sialyltransferases are tissue-specific and are involved in tissue-specific sialylation.[108] For instance, sialyltransferases carrying out α(2,6)-linkage are expressed in an exceptionally high level in tissues like the liver and have lower expression in others like skeletal muscle.[108] Then, it is possible that the cells used in this study (HEK cells, derived from Human Embryonic Kidney) present a higher expression of α(2,6)-sialyltransferases than α(2,3)-sialyltransferases, leading to lower MFI levels with SiaFind α(2,3)-specific solution when the *GNE* gene is KO.

In spite of this, a 5-fold MFI increase with PNA staining was found in HEK 293 *GNE* KO cells (**Figure 8B**).

Considering the structures recognized by the lectins analysed herein, our results are in accordance with what was expected after a *GNE* KO. Moreover, a similar trend has been typically observed in the muscle biopsies from GNEM patients.[106,107]

Unlike α(2,3)- and α(2,6)-sialylated glycans that are easily detected by lectin staining, no lectins are available to detect polysialic acid. Polysialic acid caps terminal sialic residues on N- and O-glycoproteins, like NCAM, through the action of polysialyltransferases.[109] There is evidence that polysialic acid has a role in cell adhesion, migration, synaptic plasticity, development, regeneration, immune function and disease.[110,111] In order to evaluate the polysialylation profile in the HEK 293 WT and HEK 293 *GNE* KO cells an anti-polysialic acid antibody, the 735 antibody, was used (**Figure 9**).

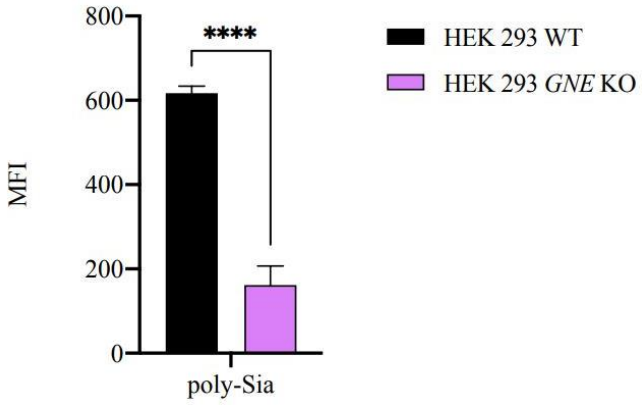

Figure 9 – Characterization of polysialylation through antibody staining. Staining of HEK 293 WT and HEK 293 GNE KO cells with 735 antibody against polysialic acid (poly-Sia). For each condition at least 1×10^4 events corresponding to the relative size and granularity of HEK 293 cells were acquired on an Attune Acoustic Focusing Cytometer using the gating strategy depicted in Figure 7. Values represent MFI (mean ± SD). Significant differences at **** $p < 0.0001$ ($n \geq 3$).

As it can be seen (**Figure 9**), polysialylation is significantly lower in *GNE* KO cells compared to WT. Altogether, the results obtained (**Figures 8** and **9**) confirm the interruption of sialic acid biosynthesis in HEK 293 *GNE* KO cell line and pinpoint this cell line as a good model to study GNEM mechanisms.

3.1.2 Metabolism of HEK 293 *GNE* KO cells

HEK 293 metabolism was evaluated during 4 h by measuring the conversion of resazurin to resorufin (**Figure 10**). The measured resorufin absorbance is directly proportional to cell viability and metabolization.

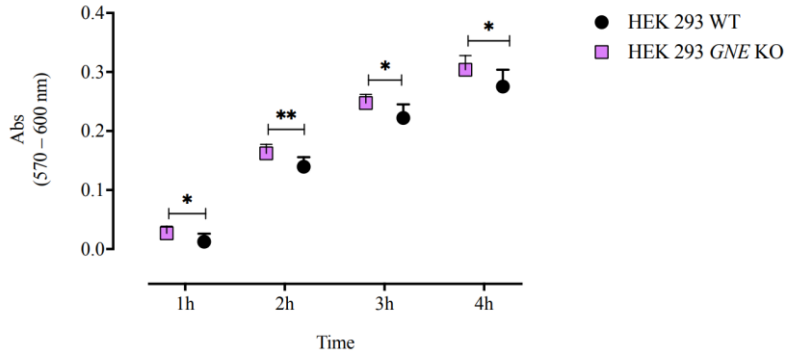

Figure 10 – Metabolization of HEK 293 cells. Measurement of metabolic activity by discount the unconverted resazurin background at 600 nm to the resorufin (product) absorbance at 570 nm. Values are treated as mean ± SD. Significant differences at * $p < 0.05$ ** $p < 0.01$ (n=3).

The metabolization measured for HEK 293 *GNE* KO cells was higher than that of HEK 293 WT (**Figure 10**). HEK 293 *GNE* KO cells converted the resazurin into resorufin more rapidly, indicating the presence of a reducing environment, typically associated with cell growth. Our results corroborate other reports, pointing to higher proliferation rate in desialylated cells, and to an inverse correlation between GNE levels and cell proliferation.[112,113]

3.2 Evaluation of an Immune Response

In order to test our hypothesis that defective sialylation in GNEM cells has an impact on the immune response, we measured the expression of MHC-I, an antigen-presenting molecule expressed by all nucleated cells. In a previous work from our group it was reported that MHC-I molecule is commonly sialylated in α(2,6).[81] Since MHC-I is essential for T cell activation and for assembling a correct immune response, we decided to investigate if the expression of this molecule was altered when the sialic biosynthesis pathway has been compromised by the *GNE* KO (**Figure 11**).

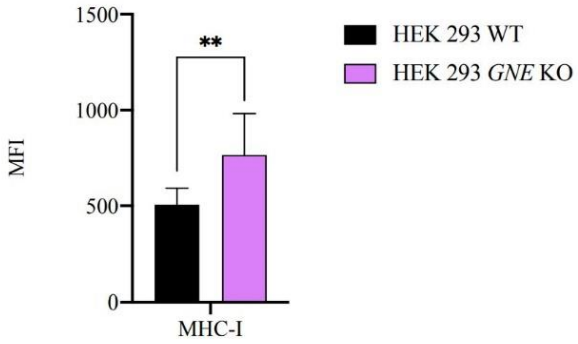

Figure 11 – Evaluation of cell surface MHC-I expression. Staining of HEK 293 WT and HEK 293 GNE KO cells with FITC conjugated anti-HLA-ABC (W6/32) antibody. For each condition at least 1×10^4 events corresponding to the relative size and granularity of HEK 293 cells were acquired on an Attune Acoustic Focusing Cytometer using the gating strategy depicted in Figure 7. Values represent MFI (mean ± SD). Significant differences at ** $p < 0.01$ ($n \geq 3$).

A significant increase in the MHC-I expression was found on the HEK 293 *GNE* KO cell surface relative to the HEK 293 WT cells (**Figure 11**). This observation is in agreement with previous data obtained after DCs desialylation, supporting that sialic acid content modulates the presence and stability of the MHC-I complex, which in turn increases antigen presentation and immune potency.[81] In this line of thinking, higher expression of MHC-I in HEK 293 *GNE* KO cells suggests the involvement of an immune response initiated *via* MHC-I presentation in GNEM. However, to confirm the previous theory, it would be important to demonstrate that this increase in MHC-I expression is reflected in increased activity of the molecule. In other words, that the increase in MHC-I results in greater antigen presentation to T lymphocytes.

Nevertheless, the higher expression of MHC-I in the GNEM cell model is consistent with some observations of infiltration of inflammatory cells with increased expression of MHC-I in muscle biopsies of early-stage GNEM patients.[79,80] Our results together with the case reports highlight the importance of studying immune mechanisms in this myopathy, especially because very little has been explored and is known.

Having in mind the need to explore other immune responses in GNEM, IL-6, IL-1β and IL-10 cytokine production by HEK 293 WT and HEK 293 *GNE* KO cells was evaluated throw ELISA assay. For IL-1β and IL-10 cytokines no signal was detected, indicating none or low secretion of these cytokines. Thus, only IL-6 levels will be discussed in this section (**Figure 12**). IL-6 cytokine is typically produced by monocytes and macrophages after recognition of PAMPs or DAMPS by the PRRs.[114] In case of an infection or injury the serum levels of IL-6 raises, and this cytokine plays several roles like activation of hepatocytes, immune-competent and haematological cells, for elimination of infectious agents and tissue healing.[114]

Among known immune-related *stimuli*, IFNγ was the one selected for simulating an infection environment in HEK 293 cells. IFNγ is a cytokine primarily produced by the cells of the immune system after the activation of PRRs or other reactive antigen receptors during infection or damage. So, an early burst of IFNγ production occurs typically during infections before the emergence of an acquired immune response.[115] However, IFNγ receptor is not exclusively expressed in immune cells but in almost all cell types, thus making IFNγ a good stimulus for the cells used in this study.[116]

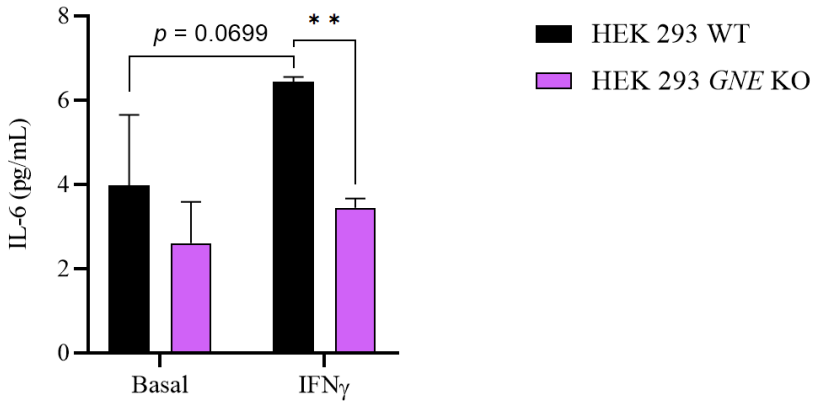

Figure 12 – IL-6 secretion in GNEM cell model. Values represent pg of IL-6 secreted per mL of HEK 293 cell supernatant (mean ± SD) at basal state and after 6 h incubation with recombinant human interferon γ (IFNγ). HEK 293 cells were cultured in DMEM medium for 24 h and incubated with DCCM-1 with or without IFNγ stimulus. Cell supernatant of each condition was collected, and IL-6 was quantified using the human IL-6 ELISA kit from ImmunoTools. P-value presented was obtained by unpaired t-test between HEK 293 WT basal and HEK 293 WT IFNγ.

As depicted in **Figure 12**, the basal levels of IL-6 released by HEK 293 WT cells are in the range of IL-6 levels already reported in the absence of stress, like injury and infections (≤ 4 pg/mL),[114] which validates our results. Considering the two cell lines evaluated, HEK 293 *GNE* KO cells exhibit lower basal levels of the cytokine in the supernatant than the HEK 293 WT cells. Moreover, when the inflammatory stimulus IFNγ was added to the cells, the value of IL-6 secreted remained almost the same for HEK 293 *GNE* KO cells while in HEK 293 WT cells an increase was observed (p = 0.0699).

The mechanism of how changes in glycosylation influence IL-6 secretion remains unclear; however, a similar trend has already been observed by our group for the most common CDG, PMM2-CDG (unpublished data). PMM2-CDG is characterized by a defect in the synthesis of N-glycans, while GNEM is associated with a defect in the sialic acid biosynthesis that compromises the addition of this sugar to N- and O-glycans. Therefore, changes in glycosylation in these two pathological conditions are considerably different, raising a question: what disturbance in glycosylation affects the secretion of IL-6?

When analysing the IL-6 and MHC-I results obtained herein, they appear to be contradictory. MHC-I result suggests a higher antigen-presentation to T lymphocytes in GNEM cells leading to the activation of a cytotoxic response, whereas IL-6 result points to lower response of GNEM cells to an infection stimulus compromising the assembling of an immune response to an infection or injury. Nevertheless, the immune system is highly complex, the same molecule can play redundant and pleiotropic functions and more than one pathway, even with opposite functions, can be active at the same time to ensure the equilibrium of the immune response. So, what the

previous results show us is that the immune response is modulated by the sialic acid content and that understanding this mechanism could bring some light into GNEM pathophysiology.

3.3 Supplementation with Intermediates of Sialic Acid Biosynthesis

With the purpose of finding a new and improved therapeutic approach for GNEM, the ProDGNE project is developing prodrugs that have ManNAc-6-P as active compound. In this work, HEK 293 WT and HEK 293 *GNE* KO cells were supplemented with ManNAc (in phase 2 clinical trial, ClinicalTrials.gov NCT04231266) and ManNAc-6-P, both intermediates of sialic acid biosynthesis, and cell toxicity and efficacy was evaluated.

3.3.1 Cell Viability Evaluation After ManNAc and ManNAc-6-P Supplementation

The cell toxicity of ManNAc and ManNAc supplementation was evaluated in HEK 293 and HepG2 cells (**Figure 13**).

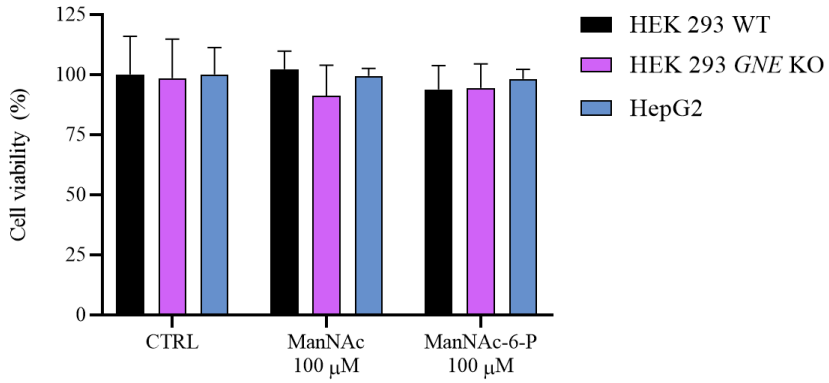

Figure 13 – Cell Viability after ManNAc and ManNAc-6-P supplementation. Cell viability measured by resazurin assay after 24 h supplementation with ManNAc (100 μM) and ManNAc-6-P (100 μM) in DCCM-1 medium. The results of cell viability were expressed as the % of resazurine reduction of treated cells relative to control (CTRL, untreated cells): Resazurine reduction (%) = (*A*compound / *A*control) × 100%, where *A* corresponds to the absorbance. Values are treated as mean ± SD (n=3).

Supplementation with ManNAc (100 μM) and ManNAc-6-P (100 μM) reveal no toxicity to HEK 293 cells (viability > 90%) (**Figure 13**), enabling evaluation of an improvement in the response of HEK 293 *GNE* KO cells after supplementation.

Assessment of cell viability in HepG2 cells after exposition to the compounds was important as ManNAc and prodrugs will be administered orally in patients. Supplementation with these concentrations of ManNAc and ManNAc-6-P did not show to reduce cell viability in a human hepatic cell line (**Figure 13**).

3.3.2 Sialophenotype After ManNAc and ManNAc-6-P Supplementation

To evaluate the effectiveness of ManNAc and ManNAc-6-P supplementation in restoring the sialic acid content at the cell surface, HEK 293 WT and HEK 293 *GNE* KO cells were stained with SiaFind α(2,3)- and α(2,6)-specific solutions, SNA and PNA, and analysed by flow cytometry (**Figure 14**).

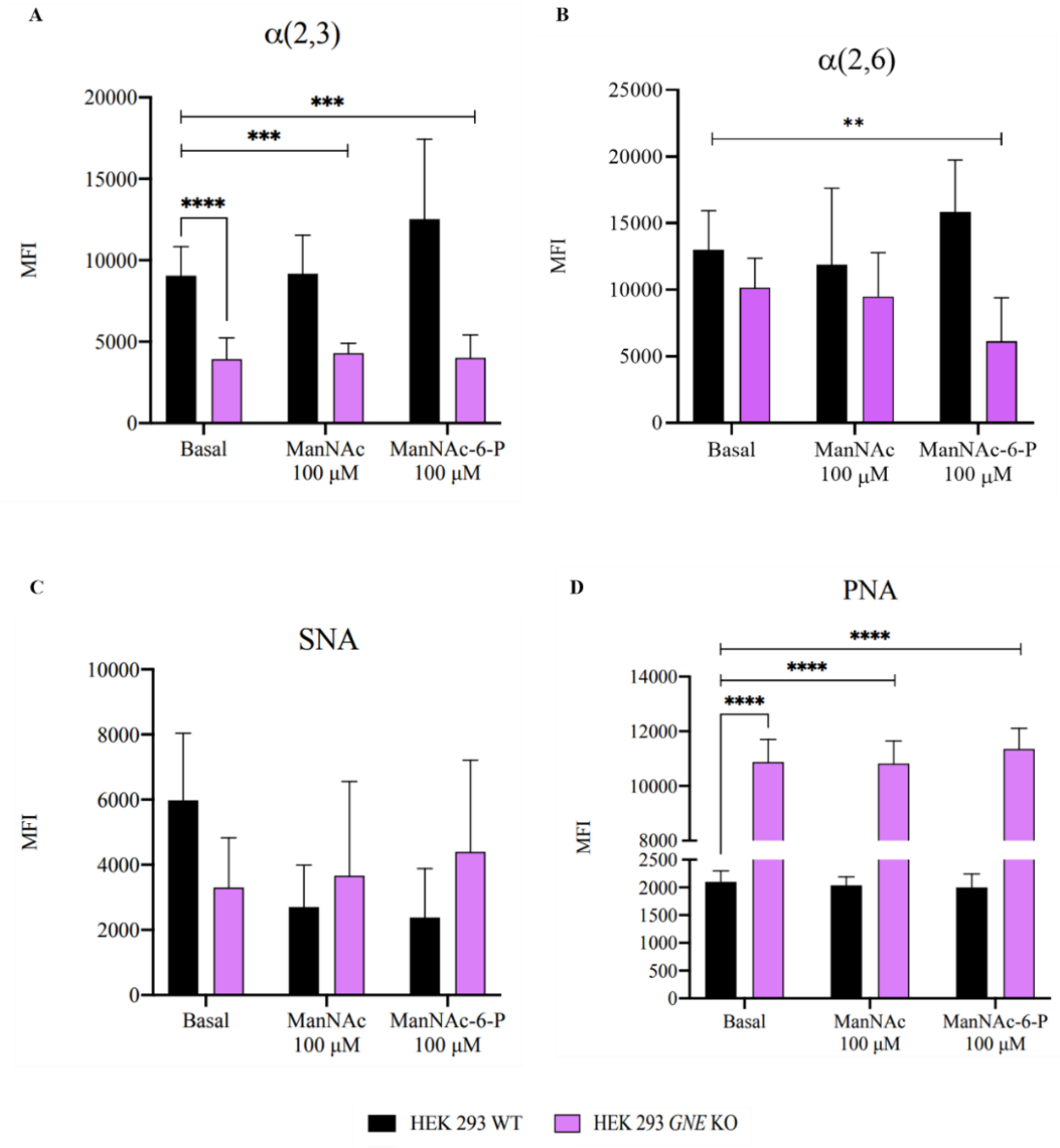

Figure 14 – Sialic acid profile after ManNAc and ManNAc-6-P supplementation. (A) SiaFind α(2,3)-specific staining (**B**) SiaFind α(2,6)-specific staining (**C**) SNA staining (**D**) PNA staining of HEK 293 WT and HEK 293 *GNE* KO cells after supplementation with ManNAc (100 µM) and ManNAc-6-P (100 µM). For each condition at least 1 × 10^4 events corresponding to the relative size and granularity of HEK 293 cells were acquired on an Attune Acoustic Focusing Cytometer using the gating strategy depicted in Figure 7. Values represent MFI (mean ± SD). Significant differences at ** $p < 0.01$, *** $p < 0.001$ and **** $p < 0.0001$($n \geq 3$) relative to HEK 293 WT basal.

Regarding SiaFind α(2,3) staining (**Figure 14A**), as in the 3.1.1 section, HEK 293 *GNE* KO cells have a lower staining then HEK 293 WT. However, when supplemented with noncytotoxic concentrations of ManNAc (100 μM) and ManNAc-6-P (100 μM), a slight increase in SiaFind α(2,3) staining of HEK 293 *GNE* KO cells was observed. This trend is depicted by a reduction in statistical significance (from **** $p < 0.0001$ to *** $p < 0.001$) when comparing the supplemented HEK 293 *GNE* KO with the basal HEK 293 WT cells. This result supports the hypothesis that supplementation with intermediates of the sialic acid pathway can improve the sialylation at the cell surface; however, a higher dose of the compounds could restore the sialophenotype.

Concerning α(2,6)-sialylation, evaluated using the SiaFind α(2,6)-specific solution (**Figure 14B**) and SNA lectin (**Figure 14C**), no conclusion can be draw. ManNAc and ManNAc-6-P supplementation resulted in a decrease of SiaFind α(2,6)-specific staining and an increase of SNA staining in HEK 293 *GNE* KO cells. These contrasting results may be due to high variability between assays and with SNA, in particular, the discrepancy between assays can be associated with the cell toxicity.

Results with PNA staining after supplementation failed to show a significant change in the sialylation profile of HEK 293 cells (**Figure 14D**).

Overall, supplementation did not show to increase cell sialylation. Although, this was not the expected results, especially for ManNAc supplementation (phase 2 clinical trials and moving forward), other works have already raised the hypothesis that intermediates of the sialic acid biosynthesis could have additional functions and be important for other pathways rather than sialic acid synthesis.[117] In any case, if the compounds participate in other cellular mechanisms, it is possible that higher doses can restore sialic acid levels. In addition, and since different cells have specific cellular mechanisms and sialylation profiles, other cell models, such as skeletal muscle cells (mainly affected in GNEM) could be used.

3.3.3 Immune Response after ManNAc and ManNAc-6-P Supplementation

To assess if supplementation with sialic acid intermediates alters the immune response, the markers MHC-I and IL-6 cytokine were measured after incubating the HEK 293 WT and HEK 293 *GNE* KO cells with ManNAc and ManNAc-6-P for 24 h. The MHC-I expression at cell surface was evaluated by flow cytometry (**Figure 15**) and IL-6 secretion was measured on supernatants by the ELISA method (**Figure 16**), as before.

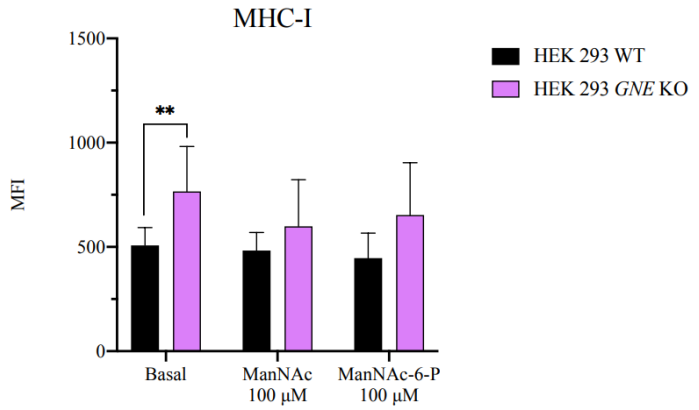

Figure 15 – MHC-I expression after ManNAc and ManNAc-6-P supplementation. Staining of HEK 293 WT and HEK 293 *GNE* KO cells with FITC conjugated anti-HLA-ABC (W6/32) antibody after supplementation with ManNAc (100 µM) and ManNAc-6-P (100 µM). For each condition at least 1×10^4 events corresponding to the relative size and granularity of HEK 293 cells were acquired on an Attune Acoustic Focusing Cytometer using the gating strategy depicted in Figure 7. Values represent MFI (mean ± SD). Significant differences at ** $p < 0.01$ ($n \geq 3$).

A decrease of MHC-I expression in HEK 293 *GNE* KO cells after supplementation with ManNAc and ManNAc-6-P was observed (**Figure 15**). In fact, the values of MFI after supplementation were lower and closer to those obtained for WT cells, suggesting that sialic acid intermediates can influence the stability of MHC-I complex, probably by promoting the turnover of the complex.

However, it is still not possible to determine if supplementation was enough to restore the sialylation of MHC-I and to conclude that the decrease in the MHC-I expression is due to sialylation of the complex. Supplementation with ManNAc and ManNAc-6-P may be affecting the stability of the MHC-I molecule *via* other pathways. To test if the sialylation of the MHC-I molecule was restored, the next step will be detecting the sialic acid content of the immunoprecipitated MHC-I protein by western blot.

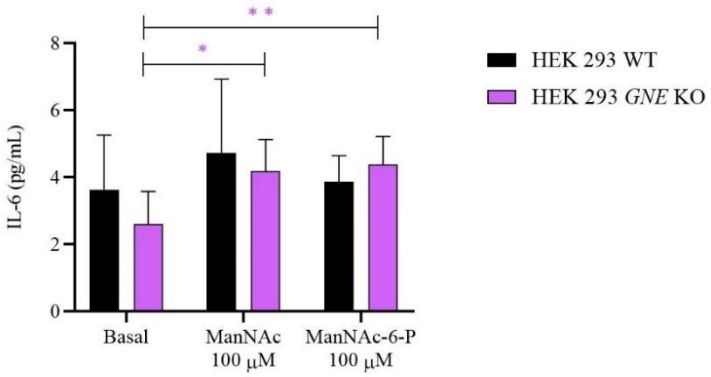

Figure 16 – IL-6 secretion in GNEM cell model. Values represent pg of IL-6 secreted per mL of medium (mean ± SD) HEK 293 cells were cultured in DMEM medium for 24 h and incubated with DCCM-1 with or without ManNAc (100 µM) and ManNAc-6-P (100 µM). The supernatant of each condition was collected, and IL-6 was quantified using the human IL-6 ELISA kit from ImmunoTools. Significant differences at * $p < 0.05$, ** $p < 0.01$ relative to basal HEK 293 GNE KO ($n \geq 3$).

Regarding IL-6 secretion (**Figure 16**), the levels of this cytokine measured in the supernatant of HEK 293 *GNE* KO cells after ManNAc and ManNAc-6-P supplementation raised significantly face to the basal levels. After supplementation, the levels of IL-6 were similar to those observed in WT cells and reported for normal cells in the absence of stress.[114] This observation suggests that supplementation with intermediates of sialic acid biosynthesis pathway can re-establish a normal IL-6 response in GNEM cells, which will be essential to fight new infections or injuries.

3.4 Prediction of ADMET-related Endpoints of Synthesized ManNAc Phosphoramidate Prodrugs

Optimal prodrugs need to have effective ADMET features, and to have appropriate safety.[118] Considering that the cost of drug development is many times larger than that of drug discovery, predictive methodologies arise as valuable tools that ultimately can aid the selection of the most promising drug candidates. Herein, we aimed at establishing a comprehensive analysis on the most appropriate phosphoramidate motifs for developing prodrugs (**Figure 17**) that meet the following requirements: a) be orally available; b) survive the gastrointestinal (GI) tract; c) be absorbed across intestinal mucosa; d) be delivered into the systemic circulation following its passive transport; and e) be distributed into cells to be converted to ManNAc-6-P, which will be directly converted into sialic acid.

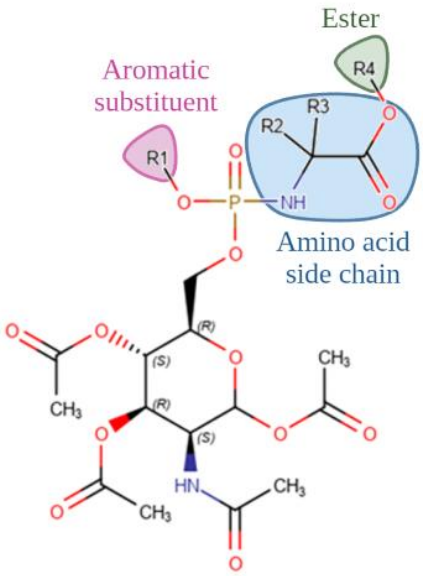

Figure 17 – ManNAc phosphoramidate prodrug template. The ManNAc-6-P molecule was used as template for the synthesis of the new prodrugs by adding phosphate masking groups.

Molecular properties and ADMET-related parameters of the synthesized ManNAc phosphoramidate prodrugs (**1**–**12**) are presented in **Table 1**.

Among others, LogP and TPSA are important physicochemical descriptors that have recognized impact on oral bioavailability of drugs[119] and in the transport across the intestinal barrier.

The TPSA of the prodrugs were all greater than 140, suggesting that they still have strong polarity and are not easily absorbed by the body. However, many compounds do not show only simple passive diffusion, being also affected by active carriers, efflux mechanisms involving P-glycoprotein (P-gp) and other transporter proteins, and gut wall metabolism.[120] In fact, the synthetized prodrugs are predicted to interact with P-gp and to be substrates of cytochrome (CYP)3A4 (**Table 1**). Although CYP3A4 and P-gp have opposite distribution patterns and expression along the human small intestine, they both display similar substrate specificities and are involved in many drug interactions.[120] Due to the significant impact of P-gp and CYP3A4 on ADMET, docking studies are proposed to understand the interaction between the prodrugs and these proteins.

The ProTide technology employs phosphate-masking groups capable of providing more favourable drug-like properties to the substrate to which is attached, such as ManNAc-6-P. Except for prodrug **3** (LogP = 0.92), the remaining ManNAc phosphoramidate prodrugs are predicted as having ideal lipophilicity ($1 \leq \text{LogP} \leq 5$) (**Table 1**). Indeed, it is reported that prodrug **3** did not demonstrate activation following the carboxypeptidase assay and it was not capable of producing observable effects on cell sialic acid levels,[101] which supports our general predictions. When compared with ManNAc (LogP = -1.76) (**Table 2**), currently in phase II of clinical trials, all prodrugs show better lipid solubility (higher LogP and lower water solubility) that may help them to interact with cell membranes.

Factors like water solubility, membrane permeability indicated by human colorectal adenocarcinoma (Caco-2) cell line, intestinal absorption (human), skin permeability, and P-gp substrate or inhibitor were used to predict the potential for a compound to be absorbed (**Tables 1** and **2**).

According to the model theory, a compound is considered to have high Caco-2 permeability if it has apparent permeability coefficient (Papp) values higher than 8×10^{-6} cm/s (which is translated in predicted values higher than 0.90). Although none of the synthesized prodrugs present high Caco-2 permeability (values ranging between -0.091 and 0.284) (**Table 1**) they are predicted to be more easily absorbed than ManNAc (log Papp = -0.285) (**Table 2**).

A molecule with an intestinal absorption of less than 30% is considered to be poorly absorbed. All prodrugs are predicted to have a good absorption (ranging between 58% and 78%) (**Table 1**), whereas ManNAc do not reach 20% absorption (**Table 2**). In fact, in the open-label, phase 2 study to evaluate oral ManNAc in 12 patients with GNEM, gastrointestinal adverse events were common and suggested to be related to an incomplete absorption of ManNAc, which supports these predictions. Still, an alternative route of administration for both the prodrugs and ManNAc can be sought (e.g., transdermal drug delivery), since they are predicted to be capable of penetrating the skin (log Kp < -2.5) (**Tables 1** and **2**).

The distribution volume (VDss), fraction unbound (human), central nervous system (CNS) permeability and blood-brain barrier (BBB) membrane permeability (log BB) were used to characterize the distribution of compounds (**Tables 1** and **2**).

Among the synthesized prodrugs, **6**, **11**, and **12** were the ones with higher distribution volume (log VDss > -0.15), but still lower than that of ManNAc (**Table 2**). In the phase 2 clinical trial ManNAc was found to be rapidly absorbed and exhibited a high apparent volume of distribution, consistent with extensive distributions to tissues,[95] which is in agreement with these predictions. Still, the capacity of both the prodrugs and ManNAc to be distributed in the brain (log BB < -1) and to penetrate the CNS (log PS < -3) is low (**Tables 1** and **2**). For prodrugs, the predicted fraction that would be unbound in plasma (ranging between 0 and 0.269 Fu) is much lower than that calculated for ManNAc (0.869 Fu), indicating that the prodrugs can cross cell membrane more efficiently than ManNAc (**Tables 1** and **2**).

The interaction with hepatic CYP enzymes, which play key roles in metabolic processes, was used to determine the putative metabolism of compounds (**Tables 1** and **2**). As mentioned before, all prodrugs are predicted to be substrates of CYP3A4 (**Table 1**), responsible for the metabolism of more than 50% of drugs, which suggests they may be metabolized in the liver.

Total clearance, corresponding to the sum of renal and hepatic processes by which drugs are removed from the body or inactivated, and assessing a compound potential to be transported by organic cation transporter 2 (OCT2), were the predictors used to characterize the excretion of compounds (**Tables 1 and 2**). Among the synthesized prodrugs, the total clearance of the prodrug **4** is predicted to be the highest (**Table 1**); however, it is still lower than that of ManNAc (**Table 2**), suggesting that ManNAc is removed from the body more rapidly than the prodrugs.

The prediction of toxicity of drug candidates is one of the important components of the drug discovery pipeline. Parameters such as mutagenicity (AMES test), cardiotoxicity (human Ether-

a-go-go-related (hERG) inhibition), hepatotoxicity and skin sensitization were selected to estimate the toxicological potential of the compounds (**Tables 1** and **2**).

Overall, the results suggest that most prodrugs may be well tolerated; however, prodrug **6** is highlighted as potentially mutagenic (AMES toxicity: Yes), cardiotoxic (hERG II inhibitor: Yes) and hepatotoxic (Hepatotoxicity: Yes) (**Table 1**). Considering that these prodrugs may be extensively metabolized in the liver, their hepatotoxic potential cannot be set aside. Although no toxic effects are predicted for ManNAc (**Table 2**), which has also been confirmed in the phase 2 clinical trial, mild transaminase elevations were observed in 75% of GNEM patients,[95] emphasizing the relevance of exploring the interaction with hepatic enzymes and monitoring liver function. The hepatoxicity potential of ManNAc (100 μM) and ManNAc-6-P (100 μM) was assessed using a cell model from hepatoblastoma, the HepG2 cell line (subsection 3.3.1). The results obtained with this cell model confirmed the absence of hepatoxicity after ManNAc and ManNAc-6-P supplementation, presenting an experimental validation for the computational predictions.

Table 1 – Results of ADMET-related properties of ManNAc phosphoramidate prodrugs with pkCSM.[a]

	PRODRUG	1	2	3	4	5	6	7	8	9	10	11	12
Molecular properties	**LogP**	1.38	1.84	0.92	1.34	2.28	2.91	2.50	1.95	2.38	3.00	2.02	2.59
	TPSA	200.90	200.90	192.11	200.90	200.90	200.90	200.90	200.90	200.90	200.90	200.90	200.90
Absorption	**Water solubility** (log mol/L)	-4.191	-4.029	-4.325	-4.115	-4.11	-4.252	-4.423	-3.994	-4.575	-4.397	-4.048	-4.105
	Caco-2 permeability (log P_{app} in 10^{-6} cm/s)	0.258	-0.091	0.011	0.193	-0.111	-0.075	-0.044	-0.02	-0.026	-0.051	0.257	0.284
	Intestinal absorption (human) (% absorbed)	58.293	60.508	68.149	66.365	64.259	77.628	71.683	60.556	71.487	72.425	62.683	62.334
	Skin Permeability (log Kp)	-2.735	-2.751	-2.725	-2.735	-2.741	-2.736	-2.741	-2.751	-2.743	-2.739	-2.735	-2.735
	P-glycoprotein substrate	Yes	Yes	No	Yes	Yes	Yes	Yes	Yes	Yes	Yes	Yes	Yes
	P-glycoprotein I inhibitor	Yes	Yes	Yes	Yes	Yes	Yes	Yes	Yes	Yes	Yes	Yes	Yes
	P-glycoprotein II inhibitor	No	Yes	No	Yes	Yes	Yes	Yes	Yes	Yes	Yes	No	No
Distribution	**VDss (human)** (log L/kg)	-0.358	-0.512	-0.677	-0.178	-0.359	-0.109	-0.332	-0.497	-0.518	-0.289	-0.123	-0.12
	Fraction unbound (human) (Fu)	0.167	0.23	0.269	0.079	0.137	0.082	0.058	0.254	0.091	0.054	0.142	0.000
	BBB permeability (log BB)	-1.761	-2.098	-2.57	-1.682	-1.941	-1.919	-1.957	-2.153	-2.023	-1.932	-1.702	-1.883
	CNS permeability (log PS)	-4.264	-4.132	-4.13	-4.364	-3.985	-3.838	-3.957	-4.148	-3.946	-3.939	-4.07	-4.177
Metabolism	**CYP2D6 substrate**	No	No	No	No	No	No	No	No	No	No	No	No
	CYP3A4 substrate	Yes	Yes	Yes	Yes	Yes	Yes	Yes	Yes	Yes	Yes	Yes	Yes
	CYP1A2 inhibitor	No	No	No	No	No	No	No	No	No	No	No	No
	CYP2C19 inhibitor	No	No	No	No	No	No	No	No	No	No	No	No
	CYP2C9 inhibitor	No	No	No	No	No	No	No	No	No	No	No	No
	CYP2D6 inhibitor	No	No	No	No	No	No	No	No	No	No	No	No
	CYP3A4 inhibitor	No	No	No	No	Yes	Yes	Yes	No	Yes	Yes	No	No
Excretion	**Total Clearance** (log mL/min/Kg)	0.088	0.153	0.292	0.302	0.097	0.04	0.004	0.238	-0.096	-0.028	0.244	-0.017
	Renal OCT2 substrate	No	No	No	No	No	No	No	No	No	No	No	No
Toxicity	**AMES toxicity**	No	No	No	No	No	Yes	No	No	No	No	No	No
	hERG I inhibitor	No	No	No	No	No	No	No	No	No	No	No	No
	hERG II inhibitor	No	No	No	Yes	Yes	Yes	No	No	Yes	Yes	No	Yes
	Hepatotoxicity	No	Yes	Yes	No	Yes	Yes	Yes	Yes	Yes	Yes	No	No
	Skin Sensitization	No	No	No	No	No	No	No	No	No	No	No	No

[a] Green colour was used for indicating desirable ADMET properties; Red colour was used for indicating undesirable ADMET properties. Octanol-water partition coefficient (LogP); topological polar surface area (TPSA); distribution volume (VDss); blood-brain barrier (BBB); central nervous system (CNS); organic cation transporter 2 (OCT2), human Ether-a-go-go-related (hERG).

Table 2 – Results of ADMET-related endpoints of ManNAc and ManNAc-6-P with pkCSM.[a]

	COMPOUND	ManNAc	ManNAc-6-P
Molecular properties	**LogP**	-1.76	-2.87
	TPSA	119.25	175.59
Absorption	**Water solubility** (log mol/L)	-0.818	-0.663
	Caco-2 permeability (log P_{app} in 10^{-6} cm/s)	-0.285	0.366
	Intestinal absorption (human) (% Absorbed)	19.518	24.044
	Skin Permeability (log Kp)	-3.264	-2.752
	P-glycoprotein substrate	No	No
	P-glycoprotein I inhibitor	No	No
	P-glycoprotein II inhibitor	No	No
Distribution	**VDss (human)** (log L/kg)	-0.101	0.253
	Fraction unbound (human) (Fu)	0.849	0.736
	BBB permeability (log BB)	-1.023	-1.275
	CNS permeability (log PS)	-4.382	-4.563
Metabolism	**CYP2D6 substrate**	No	No
	CYP3A4 substrate	No	No
	CYP1A2 inhibitor	No	No
	CYP2C19 inhibitor	No	No
	CYP2C9 inhibitor	No	No
	CYP2D6 inhibitor	No	No
	CYP3A4 inhibitor	No	No
Excretion	**Total Clearance** (log ml/min/kg)	0.718	0.359
	Renal OCT2 substrate	No	No
Toxicity	**AMES toxicity**	No	No
	hERG I inhibitor	No	No
	hERG II inhibitor	No	No
	Hepatotoxicity	No	No
	Skin Sensitization	No	No

[a] Green colour was used for indicating desireble ADMET properties; Red colour was used for indicating undesirable ADMET properties. N-Acetyl-D-mannosamine (ManNAc); N-Acetyl-D-mannosamine 6-phosphate (ManNAc-6-P); octanol-water partition coefficient (LogP); topological polar surface area (TPSA); distribution volume (VDss); blood-brain barrier (BBB); central nervous system (CNS); organic cation transporter 2 (OCT2), human Ether-a-go-go-related (hERG).

4 | Conclusions and Future Perspectives

There has been growing evidence of sialylation's role in human health and disease, including in the maintenance of a normal immune response. GNEM is known to have the sialic acid biosynthesis pathway impaired. Therefore, exploring the role of sialylation, as well as alternative cellular and molecular mechanisms that may lead to this disorder, is essential for developing novel therapeutics and ultimately improving patient quality of life.

Overall, the work developed under the scope of this dissertation paves the way for studying an immune involvement in GNEM, since an MHC-I overexpression and low IL-6 secretion levels (even in the presence of an inflammatory stimulus) were observed in a new GNEM cell model. Although MHC-I overexpression suggests the activation of the acquired immune response in GNEM cells, the low IL-6 secretion points to a greater susceptibility to pathogens. Nevertheless, the immune system is highly complex, and several pathways (even with opposite functions) are typically active at the same time to ensure a correct response.

After supplementation with sialic acid intermediates, no significant changes were observed in the sialophenotype of GNEM cells, but small improvements in the immune response were shown. The evaluation of the MHC-I and IL-6 levels proved then to be a more sensitive method, pointing these immune players as good biomarkers to be used in clinical development. Still, further work is needed to better clarify how MHC-I expression and IL-6 secretion relates with sialylation profile and other cellular mechanisms involved in GNEM.

Although no therapy is still available to fight GNEM, sialylation-increasing approaches based on prodrug technology seem to be promising. ADMET predictions conducted during this thesis suggest prodrugs to be more lipophilic, with higher membrane and intestinal absorption, and lower clearance than the reference standard ManNAc. Despite this, there were predictions of hepatoxicity, cardiotoxicity and mutagenic potential for some of the prodrugs. According to our current computational predictions, the prodrugs with better drug-like properties are prodrugs **1** and **11**, for which high absorption and no toxic effect is expected. ADMET predictions, along with the toxicity and efficacy assays that were developed, encourage us to test the new prodrugs for future clinical applications.

5 | References

1. Hart GW. Glycosylation. Curr Opin Cell Biol. 1992;4(6):1017–23.

2. Messner P. Bacterial glycoproteins. Glycoconj J. 1997;14(1):3–11.

3. Lechner J, Wieland F. Structure and Biosynthesis of Prokaryotic Glycoproteins. Annu Rev Biochem. 1989;58:173–94.

4. Schwarz F, Aebi M. Mechanisms and principles of N-linked protein glycosylation. Curr Opin Struct Biol. 2011;21(5):576–82.

5. Van Den Steen P, Rudd PM, Dwek RA, Opdenakker G. Concepts and principles of O-linked glycosylation. Crit Rev Biochem Mol Biol. 1998;33(3):151–208.

6. Eichler J. Protein glycosylation. Curr Biol. 2019;29(7):R229–31.

7. Aebi M. N-linked protein glycosylation in the ER. Biochim Biophys Acta - Mol Cell Res. 2013;1833(11):2430–7.

8. Stanley P, Moremen KW, Lewis NE, Taniguchi N, Aebi M. N-Glycans. In: Essentials of Glycobiology. 4th Edition. 2022.

9. Bieberich E. Synthesis, Processing, and Function of N-glycans in N-glycoproteins. Adv Neurobiol. 2014;9:47–70.

10. Varki A. Biological roles of glycans. Glycobiology. 2017;27(1):3–49.

11. Magalhães A, Duarte HO, Reis CA. The role of O-glycosylation in human disease. Mol Aspects Med. 2021;79:100964.

12. Mereiter S, Balmaña M, Campos D, Gomes J, Reis CA. Glycosylation in the Era of Cancer-Targeted Therapy: Where Are We Heading? Cancer Cell. 2019;36(1):6–16.

13. Rudd PM, Elliott T, Cresswell P, Wilson IA, Dwek RA. Glycosylation and the immune system. Science. 2001;291(5512):2370–6.

14. Baum LG, Cobb BA. The direct and indirect effects of glycans on immune function. Glycobiology. 2017;27(7):619–24.

15. Nicholson LB. The immune system. Essays Biochem. 2016;60(3):275–301.

16. Delves PJ, Roitt IM. The immune system. N Engl J Med. 2000;343(1):37–49.

17. Bianchi ME. DAMPs, PAMPs and alarmins: all we need to know about danger. J Leukoc Biol. 2007;81(1):1–5.

18. Commins SP, Borish L, Steinke JW. Immunologic messenger molecules: Cytokines, interferons, and chemokines. J Allergy Clin Immunol. 2010;125(2):S53–72.

19. Alberts B, Johnson A, Lewis J. The Adaptive Immune System. In: Molecular Biology of the Cell. 4th Edition. 2002. p. 1363–422.

20. Théry C, Amigorena S. The cell biology of antigen presentation in dendritic cells. Curr Opin Immunol. 2001;13(1):45–51.

21. Alberts B, Johnson A, Lewis J. Helper T Cells and Lymphocyte Activation. In: Molecular Biology of the Cell. 4th Edition. 2002.

22. Charles A Janeway J, Travers P, Walport M, Shlomchik MJ. The humoral immune response. In: Immunobiology: The Immune System in Health and Disease. 5th Edition. 2001.

23. Sung MA, Fleming K, Chen HA, Matthews S. The solution structure of PapGII from uropathogenic *Escherichia coli* and its recognition of glycolipid receptors. EMBO Rep. 2001;2(7):621–7.

24. Corfield AP. Mucins: A biologically relevant glycan barrier in mucosal protection. Biochim Biophys Acta - Gen Subj. 2015;1850(1):236–52.

25. Boltin D, Perets TT, Vilkin A, Niv Y. Mucin function in inflammatory bowel disease: An update. J Clin Gastroenterol. 2013;47(2):106–11.

26. Kataoka HH, Yasuda M, Iyori M, Kiura K, Narita M, Nakata T, et al. Roles of N-linked glycans in the recognition of microbial lipopeptides and lipoproteins by TLR2. Cell Microbiol. 2006;8(7):1199–209.

27. Cohen M, Hurtado-Ziola N, Varki A. ABO blood group glycans modulate sialic acid recognition on erythrocytes. Blood. 2009;114(17):3668–76.

28. Rabinovich GA, van Kooyk Y, Cobb BA. Glycobiology of immune responses. Ann N Y Acad Sci. 2012;1253(1):1–15.

29. Wang TT, Maamary J, Tan GS, Bournazos S, Davis CW, Krammer F, et al. Anti-HA Glycoforms Drive B Cell Affinity Selection and Determine Influenza Vaccine Efficacy. Cell. 2015;162(1):160–9.

30. van Kooyk Y, Rabinovich GA. Protein-glycan interactions in the control of innate and adaptive immune responses. Nat Immunol. 2008;9(6):593–601.

31. Blasius AL, Cella M, Maldonado J, Takai T, Colonna M. Siglec-H is an IPC-specific receptor that modulates type I IFN secretion through DAP12. Blood. 2006;107(6):2474–6.

32. Bornhöfft KF, Goldammer T, Rebl A, Galuska SP. Siglecs: A journey through the evolution of sialic acid-binding immunoglobulin-type lectins. Dev Comp Immunol. 2018;86:219–31.

33. Leffler H, Carlsson S, Hedlund M, Qian Y, Poirier F. Introduction to galectins. Glycoconj J. 2004;19(7–9):433–40.

34. Rabinovich GA, Toscano MA, Ilarregui JM, Rubinstein N. Shedding light on the immunomodulatory properties of galectins: Novel regulators of innate and adaptive immune responses. Glycoconj J. 2004;19(7–9):565–73.

35. Zuñiga E, Rabinovich GA, Iglesias MM, Gruppi A. Regulated expression of galectin-1 during B-cell activation and implications for T-cell apoptosis. J Leukoc Biol. 2001;70(1):73–9.

36. Almkvist J, Karlsson A. Galectins as inflammatory mediators. Glycoconj J. 2004;19(7–9):575–81.

37. Takenaka Y, Fukumori T, Raz A. Galectin-3 and metastasis. Glycoconj J. 2004;19(7–9):543–9.

38. Weis WI, Taylor ME, Drickamer K. The C-type lectin superfamily in the immune system. Immunol Rev. 1998;163:19–34.

39. Verheijen J, Tahata S, Kozicz T, Witters P, Morava E. Therapeutic approaches in Congenital Disorders of Glycosylation (CDG) involving N-linked glycosylation: an update. Genet Med. 2020;22(2):268–79.

40. Chang IJ, He M, Lam CT. Congenital Disorders of Glycosylation. Ann Transl Med. 2018;6(24):1–13.

41. Freeze HH, Aebi M. Altered glycan structures: The molecular basis of congenital disorders of glycosylation. Curr Opin Struct Biol. 2005;15(5):490–8.

42. Ng BG, Freeze HH. Perspectives on Glycosylation and Its Congenital Disorders. Trends Genet. 2018;34(6):466–76.

43. Pajusalu S, Vals MA, Mihkla L, Šamarina U, Kahre T, Õunap K. The Estimated Prevalence of N-Linked Congenital Disorders of Glycosylation Across Various Populations Based on Allele Frequencies in General Population Databases. Front Genet. 2021;12:1–6.

44. Schollen E, Kjaergaard S, Legius E, Schwartz M, Matthijs G. Lack of Hardy-Weinberg equilibrium for the most prevalent PMM2 mutation in CDG-Ia (congenital disorders of glycosylation type Ia). Eur J Hum Genet. 2000;8(5):367–71.

45. Brasil S, Pascoal C, Francisco R, Marques-da-Silva D, Andreotti G, Videira PA, et al. CDG therapies: From bench to bedside. Int J Mol Sci. 2018;19(5):1304.

46. Argov Z, Yarom R. "Rimmed vacuole myopathy" sparing the quadriceps. A unique disorder in iranian jews. J Neurol Sci. 1984;64(1):33–43.

47. Nonaka I, Sunohara N, Ishiura S, Satoyoshi E. Familial distal myopathy with rimmed vacuole and lamellar (myeloid) body formation. J Neurol Sci. 1981;51(1):141–55.

48. Eisenberg I, Avidan N, Potikha T, Hochner H, Chen M, Olender T, et al. The UDP-N-acetylglucosamine 2-epimerase/N-acetylmannosamine kinase gene is mutated in recessive hereditary inclusion body myopathy. Nat Genet. 2001;29(1):83–7.

49. Nishino I, Noguchi S, Murayama K, Driss A, Sugie K, Oya Y, et al. Distal myopathy with rimmed vacuoles is allelic to hereditary inclusion body myopathy. Neurology. 2002;59(11):1689–93.

50. Huizing M, Carrillo-Carrasco N, Malicdan MC V, Noguchi S, Gahl WA, Mitrani-Rosenbaum S, et al. GNE myopathy: new name and new mutation nomenclature. Neuromuscul Disord. 2014;24(5):387–9.

51. Pogoryelova O, Cammish P, Mansbach H, Argov Z, Nishino I, Skrinar A, et al. Phenotypic stratification and genotype-phenotype correlation in a heterogeneous, international cohort of GNE myopathy patients: First report from the GNE myopathy Disease Monitoring Program, registry portion. Neuromuscul Disord. 2018;28(2):158–68.

52. Slota C, Bevans M, Yang L, Shrader J, Joe G, Carrillo N. Patient reported outcomes in GNE myopathy: incorporating a valid assessment of physical function in a rare disease. Disabil Rehabil. 2017;40(10):1206–13.

53. Ishihara S, Tomimitsu H, Fujigasaki H, Saito F, Mizusawa H. UDP-N-acetylglucosamine 2-epimerase/N-acetylmannosamine kinase in nuclei and rimmed vacuoles of muscle fibers in DMRV (distal myopathy with rimmed vacuoles). J Med Dent Sci. 2008;55(1):181–7.

54. Argov Z. GNE myopathy: a personal trip from bedside observation to therapeutic trials. Acta Myol. 2014;33(2):107–10.

55. Pogoryelova O, González Coraspe JA, Nikolenko N, Lochmüller H, Roos A. GNE myopathy: from clinics and genetics to pathology and research strategies. Orphanet J Rare Dis. 2018;13(70):1–15.

56. Schwarzkopf M, Knobeloch KP, Rohde E, Hinderlich S, Wiechens N, Lucka L, et al. Sialylation is essential for early development in mice. Proc Natl Acad Sci U S A. 2002;99(8):5267–70.

57. Nishino I, Carrillo-Carrasco N, Argov Z. GNE myopathy: current update and future therapy. J Neurol Neurosurg Psychiatry. 2015;86(4):385–92.

58. Celeste F V, Vilboux T, Ciccone C, de Dios JK, Malicdan MC V, Leoyklang P, et al. Mutation update for *GNE* gene variants associated with GNE myopathy. Hum Mutat. 2014;35(8):915–26.

59. Kaback M, Lopatequi J, Portuges AR, Quindipan C, Pariani M, Salimpour-Davidov N, et al. Genetic screening in the Persian Jewish community: A pilot study. Genet Med. 2010;12(10):628–33.

60. Ohno K. Mutation analysis of a large cohort of GNE myopathy reveals a diverse array of *GNE* mutations affecting sialic acid biosynthesis. J Neurol Neurosurg Psychiatry. 2014;85(8):831.

61. Kalaydjieva L, Lochmüller H, Tournev I, Baas F, Beres J, Colomer J, et al. 125th ENMC International Workshop: Neuromuscular disorders in the Roma (Gypsy) population, 23-25 April 2004, Naarden, The Netherlands. Neuromuscul Disord. 2005;15(1):65–71.

62. Nalini A, Gayathri N, Nishino I, Hayashi YK. GNE myopathy in India. Neurol India. 2013;61(4):371–4.

63. Liewluck T, Pho-Iam T, Limwongse C, Thongnoppakhun W, Boonyapisit K, Raksadawan N, et al. Mutation analysis of the *GNE* gene in distal myopathy with rimmed vacuoles (DMRV) patients in Thailand. Muscle Nerve. 2006;34(6):775–8.

64. Zhu W, Mitsuhashi S, Yonekawa T, Noguchi S, Huei JCY, Nalini A, et al. Missing genetic variations in GNE myopathy: rearrangement hotspots encompassing 5'UTR and founder allele. J Hum Genet. 2017;62(2):159–66.

65. Carrillo N, Malicdan MC, Huizing M. GNE Myopathy: Etiology, Diagnosis, and Therapeutic Challenges. Neurotherapeutics. 2018;15(4):900–14.

66. Cho A, Hayashi YK, Monma K, Oya Y, Noguchi S, Nonaka I, et al. Mutation profile of the *GNE* gene in Japanese patients with distal myopathy with rimmed vacuoles (GNE myopathy). J Neurol Neurosurg Psychiatry. 2014;85(8):914–7.

67. Chamova T, Guergueltcheva V, Gospodinova M, Krause S, Cirak S, Kaprelyan A, et al. GNE myopathy in Roma patients homozygous for the p.I618T founder mutation. Neuromuscul Disord. 2015;25(9):713–8.

68. Pogoryelova O, Wilson IJ, Mansbach H, Argov Z, Nishino I, Lochmüller H. GNE genotype explains 20% of phenotypic variability in GNE myopathy. Neurol Genet. 2019;5(1):e308.

69. Schauer R. Sialic acids as regulators of molecular and cellular interactions. Curr Opin Struct Biol. 2009;19(5):507–14.

70. Varki A. Diversity in the sialic acids. Glycobiology. 1992;2(1):25–40.

71. Stäsche R, Hinderlich S, Weise C, Effertz K, Lucka L, Moormann P, et al. A bifunctional enzyme catalyzes the first two steps in N-acetylneuraminic acid biosynthesis of rat liver. J Biol Chem. 1997;272(39):24319–24.

72. Kean EL, Münster-Kühnel AK, Gerardy-Schahn R. CMP-sialic acid synthetase of the nucleus. Biochim Biophys Acta - Gen Subj. 2004;1673(1–2):56–65.

73. Ricci E, Broccolini A, Gidaro T, Morosetti R, Gliubizzi C, Frusciante R, et al. NCAM is hyposialylated in hereditary inclusion body myopathy due to *GNE* mutations. Neurology. 2006;66(5):755–8.

74. Huizing M, Rakocevic G, Sparks SE, Mamali I, Shatunov A, Goldfarb L, et al. Hypoglycosylation of alpha-dystroglycan in patients with hereditary IBM due to GNE mutations. Mol Genet Metab. 2004;81(3):196–202.

75. Lochmüller H, Behin A, Caraco Y, Lau H, Mirabella M, Tournev I, et al. A phase 3 randomized study evaluating sialic acid extended-release for GNE myopathy. Neurology. 2019;92(18):e2109–17.

76. Chaudhary P, Sharma S, Singh R, Arya R. Elucidation of ER stress and UPR pathway in sialic acid-deficient cells: Pathological relevance to GNEM. J Cell Biochem. 2021;122(12):1886–902.

77. Cho A, Christine M, Malicdan V, Miyakawa M, Nonaka I, Nishino I, et al. Sialic acid deficiency is associated with oxidative stress leading to muscle atrophy and weakness in GNE myopathy. Hum Mol Genet. 2017;26(16):3081–93.

78. Hotamisligil GS. Inflammation and metabolic disorders. Nature. 2006;444:860–7.

79. Tanboon J, Rongsa K, Pithukpakorn M, Boonyapisit K, Limwongse C, Sangruchi T. A Novel Mutation of the *GNE* Gene in Distal Myopathy with Rimmed Vacuoles: A Case with Inflammation. Case Rep Neurol. 2014;6(1):55–9.

80. Krause S, Schlotter-Weigel B, Walter MC, Najmabadi H, Wiendl H, Müller-Höcker J, et al. A novel homozygous missense mutation in the *GNE* gene of a patient with quadriceps-sparing hereditary inclusion body myopathy associated with muscle inflammation. Neuromuscul Disord. 2003;13(10):830–4.

81. Silva Z, Ferro T, Almeida D, Soares H, Ferreira JA, Deschepper FM, et al. MHC class I stability is modulated by cell surface sialylation in human dendritic cells. Pharmaceutics. 2020;12(3):249.

82. Silva M, Silva Z, Marques G, Ferro T, Gonçalves M, Monteiro M, et al. Sialic acid removal from dendritic cells improves antigen cross-presentation and boosts anti-tumor immune responses. Oncotarget. 2016;7(27):41053–66.

83. Hinderlich S, Weidemann W, Yardeni T, Horstkorte R, Marjan Huizing. UDP-GlcNAc 2-Epimerase/ManNAc Kinase (GNE): A Master Regulator of Sialic Acid Synthesis.Top Curr Chem. 2013;366.

84. Galeano B, Klootwijk R, Manoli I, Sun M, Ciccone C, Darvish D, et al. Mutation in the key enzyme of sialic acid biosynthesis causes severe glomerular proteinuria and is rescued by N-acetylmannosamine. J Clin Invest. 2007;117(6):1585–94.

85. Niethamer TK, Yardeni T, Leoyklang P, Ciccone C, Astiz-Martinez A, Jacobs K, et al. Oral monosaccharide therapies to reverse renal and muscle hyposialylation in a mouse model of GNE myopathy. Mol Genet Metab. 2012;107(4):748–55.

86. Sela I, Yakovlev L, Becker Cohen M, Elbaz M, Yanay N, Ben Shlomo U, et al. Variable phenotypes of knockin mice carrying the M712T Gne mutation. Neuromolecular Med. 2013;15(1):180–91.

87. Malicdan MC V, Noguchi S, Nonaka I, Hayashi YK, Nishino I. A Gne knockout mouse expressing human *GNE* D176V mutation develops features similar to distal myopathy with rimmed vacuoles or hereditary inclusion body myopathy. Hum Mol Genet. 2007;16(21):2669–82.

88. Malicdan MC V, Noguchi S, Nonaka I, Hayashi YK, Nishino I. A Gne knockout mouse expressing human V572L mutation develops features similar to distal myopathy with rimmed vacuoles or hereditary inclusion body myopathy. Hum Mol Genet. 2007;16(2):115–28.

89. Ito M, Sugihara K, Asaka T, Toyama T, Yoshihara T, Furuichi K, et al. Glycoprotein hyposialylation gives rise to a nephrotic-like syndrome that is prevented by sialic acid administration in GNE V572L point-mutant mice. PLoS One. 2012;7(1):e29873.

90. Mitrani-Rosenbaum S, Yakovlev L, Becker Cohen M, Argov Z, Fellig Y, Harazi A. Pre Clinical Assessment of AAVrh74.MCK.GNE Viral Vector Therapeutic Potential: Robust Activity Despite Lack of Consistent Animal Model for GNE Myopathy. J Neuromuscul Dis. 2022;9(1):179–92.

91. Sparks S, Rakocevic G, Joe G, Manoli I, Shrader J, Harris-Love M, et al. Intravenous immune globulin in hereditary inclusion body myopathy: a pilot study. BMC Neurol. 2007;7:3.

92. Argov Z, Caraco Y, Lau H, Pestronk A, Shieh PB, Skrinar A, et al. Aceneuramic Acid Extended Release Administration Maintains Upper Limb Muscle Strength in a 48-week Study of

Subjects with GNE Myopathy: Results from a Phase 2, Randomized, Controlled Study. J Neuromuscul Dis. 2016;3(1):49–66.

93. Hinderlich S, Berger M, Keppler OT, Pawlita M, Reutter W. Biosynthesis of N-acetylneuraminic acid in cells lacking UDP-N-acetylglucosamine 2-epimerase/N-acetylmannosamine kinase. Biol Chem. 2001;382(2):291–7.

94. Xu X, Wang AQ, Latham LL, Celeste F, Ciccone C, Malicdan MC, et al. Safety, pharmacokinetics and sialic acid production after oral administration of N-acetylmannosamine (ManNAc) to subjects with GNE myopathy. Mol Genet Metab. 2017;122(1–2):126–34.

95. Carrillo N, Malicdan MC, Leoyklang P, Shrader JA, Joe G, Slota C, et al. Safety and efficacy of N-acetylmannosamine (ManNAc) in patients with GNE myopathy: an open-label phase 2 study. Genet Med. 2021;23(11):2067–75.

96. Mitrani-Rosenbaum S, Yakovlev L, Becker Cohen M, Telem M, Elbaz M, Yanay N, et al. Sustained expression and safety of human GNE in normal mice after gene transfer based on AAV8 systemic delivery. Neuromuscul Disord. 2012;22(11):1015–24.

97. Zygmunt DA, Crowe KE, Flanigan KM, Martin PT. Comparison of Serum rAAV Serotype-Specific Antibodies in Patients with Duchenne Muscular Dystrophy, Becker Muscular Dystrophy, Inclusion Body Myositis, or GNE Myopathy. Hum Gene Ther. 2017;28(9):737–46.

98. Wu KM. A new classification of prodrugs: Regulatory perspectives. Pharmaceuticals. 2009;2(3):77–81.

99. Keating GM, Vaidya A. Sofosbuvir: First global approval. Drugs. 2014;74(2):273–82.

100. McGuigan C, Serpi M, Bibbo R, Roberts H, Hughes C, Caterson B, et al. Phosphate prodrugs derived from N-acetylglucosamine have enhanced chondroprotective activity in explant cultures and represent a new lead in antiosteoarthritis drug discovery. J Med Chem. 2008;51(18):5807–12.

101. Morozzi C, Sedláková J, Serpi M, Avigliano M, Carbajo R, Sandoval L, et al. Targeting GNE Myopathy: A Dual Prodrug Approach for the Delivery of N-Acetylmannosamine 6-Phosphate. J Med Chem. 2019;62(17):8178–93.

102. Salama I, Hinderlich S, Shlomai Z, Eisenberg I, Krause S, Yarema K, et al. No overall hyposialylation in hereditary inclusion body myopathy myoblasts carrying the homozygous M712T *GNE* mutation. Biochem Biophys Res Commun. 2005;328(1):221–6.

103. Csepregi R, Lemli B, Kunsági-Máté S, Szente L, Koszegi T, Németi B, et al. Complex formation of resorufin and resazurin with b-cyclodextrins: Can cyclodextrins interfere with a resazurin cell viability assay? Molecules. 2018;23(2):382.

104. Tsaneva M, Van Damme EJM. 130 years of Plant Lectin Research. Glycoconj J. 2020;37(5):533–51.

105. Cummings RD, Etzler ME. Antibodies and Lectins in Glycan Analysis. In: Essentials of Glycobiology. 2nd Edition. 2009.

106. Leoyklang P, Class B, Noguchi S, Gahl WA, Carrillo N, Nishino I, et al. Quantification of lectin fluorescence in GNE myopathy muscle biopsies. Muscle Nerve. 2018;58(2):286–92.

107. Voermans NC, Guillard M, Doedée R, Lammens M, Huizing M, Padberg GW, et al. Clinical features, lectin staining, and a novel GNE frameshift mutation in hereditary inclusion body myopathy. Clin Neuropathol. 2010;29(2):71–7.

108. Awasthi K, Srivastava A, Bhattacharya S, Bhattacharya A. Tissue specific expression of sialic acid metabolic pathway: role in GNE myopathy. J Muscle Res Cell Motil. 2021;42(1):99–116.

109. Colley KJ, Kitajima K, Sato C. Polysialic acid: Biosynthesis, novel functions and applications. Crit Rev Biochem Mol Biol. 2014;49(6):498–532.

110. Schnaar RL, Gerardy-Schahn R, Hildebrandt H. Sialic acids in the brain: Gangliosides and polysialic acid in nervous system development, stability, disease, and regeneration. Physiol Rev. 2014;94(2):461–518.

111. Villanueva-Cabello TM, Gutiérrez-Valenzuela LD, Salinas-Marín R, López-Guerrero D V., Martínez-Duncker I. Polysialic Acid in the Immune System. Front Immunol. 2022;12:823637.

112. Weidemann W, Klukas C, Klein A, Simm A, Schreiber F, Horstkorte R. Lessons from GNE-deficient embryonic stem cells: Sialic acid biosynthesis is involved in proliferation and gene expression. Glycobiology. 2010;20(1):107–17.

113. Singh R, Arya R. GNE Myopathy and Cell Apoptosis: A Comparative Mutation Analysis. Mol Neurobiol. 2016;53(5):3088–101.

114. Tanaka T, Narazaki M, Masuda K, Kishimoto T. Regulation of IL-6 in immunity and diseases. In: Regulation of Cytokine Gene Expression in Immunity and Diseases Advances in Experimental Medicine and Biology. 1st Edition. 2016. p. 79–88.

115. Ivashkiv LB. IFNγ: signalling, epigenetics and roles in immunity, metabolism, disease and cancer immunotherapy. Nat Rev Immunol. 2018;18(9):545–58.

116. Rosenzweig SD, Dorman SE, Uzel G, Shaw S, Scurlock A, Brown MR, et al. A Novel Mutation in IFN-γ Receptor 2 with Dominant Negative Activity: Biological Consequences of Homozygous and Heterozygous States. J Immunol. 2004;173(6):4000–8.

117. Anke P Willems. Genetic Disorders in Sialic Acid Metabolism - A Biochemical Perspective. PhD thesis. Radboud University Nijmegen; 2019.

118. Markovic M, Ben-Shabat S, Dahan A. Prodrugs for improved drug delivery: Lessons learned from recently developed and marketed products. Pharmaceutics. 2020;12(11):1031.

119. Veber DF, Johnson SR, Cheng H-Y, Smith BR, Ward KW, Kopple KD. Molecular properties that influence the oral bioavailability of drug candidates. J Med Chem. 2002;45(12):2615–23.

120. Watanabe T, Maeda K, Nakai C, Sugiyama Y. Investigation of the Effect of the Uneven Distribution of CYP3A4 and P-Glycoprotein in the Intestine on the Barrier Function against Xenobiotics: A Simulation Study. J Pharm Sci. 2013;102(9):3196–204.

6 | Appendix

Appendix 1: Supplementary Documents

SANTA CRUZ

GLCNE CRISPR/Cas9 KO Plasmid (h): sc-406100

BACKGROUND

The Clustered Regularly Interspaced Short Palindromic Repeats (CRISPR) and CRISPR-associated protein (Cas9) system is an adaptive immune response defense mechanism used by archea and bacteria for the degradation of foreign genetic material (4,6). This mechanism can be repurposed for other functions, including genomic engineering for mammalian systems, such as gene knockout (KO) (1,2,3,5). CRISPR/Cas9 KO Plasmid products enable the identification and cleavage of specific genes by utilizing guide RNA (gRNA) sequences derived from the Genome-scale CRISPR Knock-Out (GeCKO) v2 library developed in the Zhang Laboratory at the Broad Institute (3,5).

REFERENCES

1. Cong, L., et al. 2013. Multiplex genome engineering using CRISPR/Cas systems. Science 339: 819-823.
2. Mali, P., et al. 2013. RNA-guided human genome engineering via Cas9. Science 339: 823-826.
3. Ran, F.A., et al. 2013. Genome engineering using the CRISPR-Cas9 system. Nat. Protoc. 8: 2281-2308.
4. Van der Oost, J., et al. 2014. Unraveling the structural and mechanistic basis of CRISPR-Cas systems. Nat. Rev. Microbiol. 7: 479-492.
5. Shalem, O., et al. 2014. Genome-scale CRISPR-Cas9 knockout screening in human cells. Science 343: 84-87.
6. Hsu, P., et al. 2014. Development and applications of CRISPR-Cas9 for genome editing. Cell 157: 1262-1278.

CHROMOSOMAL LOCATION

Genetic locus: GNE (human) mapping to 9p13.3.

PRODUCT

GLCNE CRISPR/Cas9 KO Plasmid (h) is designed to disrupt gene expression by causing a double-strand break (DSB) in a 5' constitutive exon within the GNE (human) gene.

GLCNE CRISPR/Cas9 KO Plasmid (h) consists of a pool of 3 plasmids, each encoding the Cas9 nuclease and a target-specific 20 nt guide RNA (gRNA) designed for maximum knockout efficiency. Each vial contains 20 µg of lyophilized CRISPR/Cas9 Plasmid DNA. Suitable for up to 20 transfections. Also see GLCNE HDR Plasmid (h): sc-406100-HDR for selection of cells containing a DSB induced by GLCNE CRISPR/Cas9 KO Plasmid (h).

STORAGE AND RESUSPENSION

Store lyophilized plasmid DNA at 4° C with desiccant. Stable for at least one year from the date of shipment. Once resuspended, store at 4° C for short term storage or -20° C for long-term storage. Avoid repeated freeze thaw cycles.

Resuspend lyophilized plasmid DNA in 200 µl of the provided ultrapure, sterile, DNase-free water. Resuspension of the plasmid DNA makes a 0.1 µg/µl solution in a 10 mM TRIS EDTA, 1 mM EDTA buffered solution.

APPLICATIONS

GLCNE CRISPR/Cas9 KO Plasmid (h) is recommended for the disruption of gene expression in human cells.

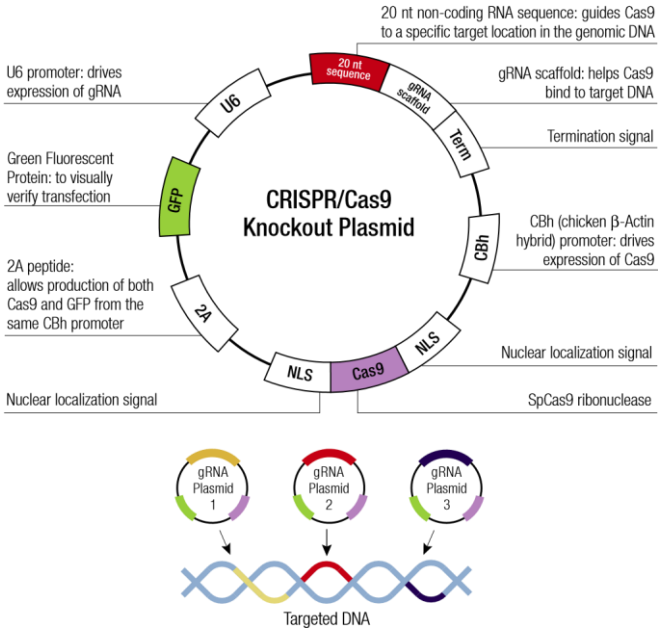

SUPPORT REAGENTS

For optimal reaction efficiency with CRISPR/Cas9 KO Plasmids, Santa Cruz

Biotechnology's UltraCruz® Transfection Reagent: sc-395739 (0.2 ml) and Plasmid Transfection Medium: sc-108062 (20 ml) are recommended. Control CRISPR/Cas9 Plasmid: sc-418922 (20 µg) negative control is also available.

GENE EXPRESSION MONITORING

GLCNE (H-10): sc-376057 is recommended as a control antibody for monitoring of GNE (human) gene expression prior to and after knockout by Western blotting (starting dilution 1:200, dilution range 1:100-1:1000) or immunofluorescence (starting dilution 1:50, dilution range 1:50-1:500).

RESEARCH USE

The CRISPR/Cas9 KO Plasmids are considered "Licensed Products" and are to be used in accordance with the Limited License stated on www.scbt.com/limitedlicense.

The purchase of this product conveys to the buyer the nontransferable right to use the purchased amount of the product and all replicates and derivatives for research purposes conducted by the buyer in his laboratory only (whether the buyer is an academic or for-profit entity). The buyer cannot sell or otherwise transfer (a) this product (b) its components or (c) materials made using this product or its components to a third party, or otherwise use this product or its components or materials made using this product or its components for Commercial Purposes.

SANTA CRUZ BIOTECHNOLOGY, INC.

GLCNE HDR Plasmid (h): sc-406100-HDR

BACKGROUND

DNA containing double-strand breaks (DSB) created by the CRISPR/Cas9 system can be repaired by either the non-homologous end-joining (NHEJ) or the homology-directed repair (HDR) pathway (1,2,3). The NHEJ repair pathway introduces non-specific insertions or deletions at the cleavage site, whereas the HDR pathway allows for precise gene editing at the DSB site (1,2,3). Target-specific HDR Plasmids provide a DNA repair template for a DSB and, when co-transfected with CRISPR/Cas9 KO Plasmids, enable the insertion of specific selection markers where Cas9-induced DNA cleavage has occurred (1,2). The HDR plasmid can incorporate a Red Fluorescent Protein (RFP) gene to visually confirm transfection and an antibiotic resistance gene (puromycin) for selection of cells containing a successful CRISPR/Cas9 doublestrand break. The puromycin resistance and RFP encoding genes are flanked by two LoxP sites that are recognized by the Cre Vector, which can be used to later remove these selection markers from the genomic DNA (4,5).

REFERENCES

1. Mali, P., et al. 2013. RNA-guided human genome engineering via Cas9. Science 339: 823-826.
2. Ran, F.A., et al. 2013. Genome engineering using the CRISPR-Cas9 system.Nat. Protoc. 8: 2281-2308.
3. Hsu, P., et al. 2014. Development and applications of CRISPR-Cas9 forgenome editing. Cell 157: 1262-1278.
4. Ma, Y. 2014. Generation of eGFP and Cre knockin rats by CRISPR/Cas9. FEBS J. 281: 3779-3790.
5. Ma, Y., et al. 2014. Generating rats with conditional alleles usingCRISPR/Cas9. Cell Res. 24: 122-125.

CHROMOSOMAL LOCATION

Genetic locus: GNE (human) mapping to 9p13.3.

PRODUCT

GLCNE HDR Plasmid (h) consists of a pool of 2-3 plasmids, each containing a homology-directed DNA repair (HDR) template corresponding to the cut sites generated by the GLCNE CRISPR/Cas9 KO Plasmid (h): sc-406100. Each HDR template contains two 800 bp homology arms designed to specifically bind to the genomic DNA surrounding the corresponding Cas9-induced doublestrand DNA break site. Each vial contains 20 µg of lyophilized HDR Plasmid DNA. Suitable for up to 20 transfections.

STORAGE AND RESUSPENSION

Store lyophilized plasmid DNA at 4° C with desiccant. Stable for at least one year from the date of shipment. Once resuspended, store at 4° C for short term storage or -20° C for long-term storage. Avoid repeated freeze thaw cycles.

Resuspend lyophilized plasmid DNA in 200 µl of the provided ultrapure, sterile, DNase-free water. Resuspension of the plasmid DNA makes a 0.1 µg/µl solution in a 10 mM TRIS EDTA, 1 mM EDTA buffered solution.

APPLICATIONS

GLCNE HDR Plasmid (h) is recommended for co-transfection with GLCNE CRISPR/Cas9 KO Plasmid (h): sc-406100 and designed for repair of the sitespecific Cas9-induced DNA cleavage within the GNE (human) gene. During repair, the GLCNE HDR Plasmid (h) incorporates a puromycin resistance gene to enable selection of stable knockout (KO) cells and an RFP gene to visually confirm transfection.

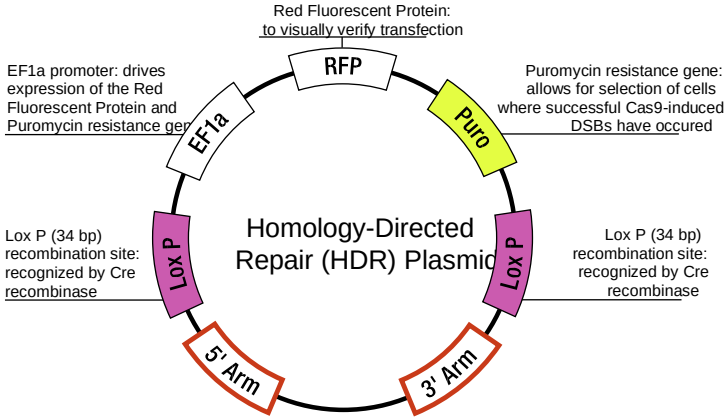

SUPPORT REAGENTS

For optimal reaction efficiency with HDR Plasmids, Santa Cruz Biotechnology's

UltraCruz® Transfection Reagent: sc-395739 (0.2 ml), Plasmid Transfection Medium: sc-108062 (20 ml) and L-755,507: sc-204045 (10 mg) are recommended. Cre Vector: sc-418923 (20 µg in 20 µl) is also available for the optional removal of the puromycin resistance gene inserted during homologydirected repair.

GENE EXPRESSION MONITORING

GLCNE (H-10): sc-376057 is recommended as a control antibody for monitoring of GNE (human) gene expression prior to and after knockout by Western blotting (starting dilution 1:200, dilution range 1:100-1:1000) or immunofluorescence (starting dilution 1:50, dilution range 1:50-1:500).

RESEARCH USE

The purchase of this product conveys to the buyer the nontransferable right to use the purchased amount of the product and all replicates and derivatives for research purposes conducted by the buyer in his laboratory only (whether the buyer is an academic or for-profit entity). The buyer cannot sell or otherwise transfer (a) this product (b) its components or (c) materials made using this product or its components to a third party, or otherwise use this product or its components or materials made using this product or its components for Commercial Purposes.

PROTOCOLS

See our web site at www.scbt.com for detailed protocols and support products.

Appendix 2: Supplementary Figures

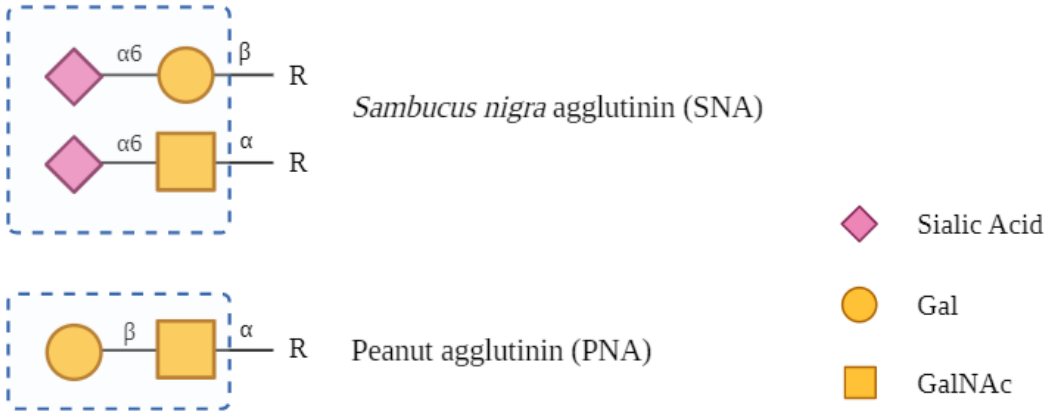

Supplementary Figure 1 – Examples of glycans that are recognized by SNA and PNA lectins. Galactose (Gal); *N*-acetylgalactosamine (GalNAc). Based on Cummings, RD. *et al.* (2009).[105]

2022

BEATRIZ L. PEREIRA

NEW INSIGHTS ON THE PATHOMECHANISM OF GNE MYOPATHY:
PROPOSING AN IMMUNE-MEDIATED RESPONSE

NOVA SCHOOL OF SCIENCE & TECHNOLOGY